The first operations of Mo.S.E. system to prevent the flooding of Venice: Insights on the hydrodynamics of a regulated lagoon

Riccardo A. Mel [a,*], Daniele P. Viero [b], Luca Carniello [b], Andrea Defina [b], Luigi D'Alpaos [b]

[a] *Department of Environmental Engineering, University of Calabria, via Pietro Bucci, 87036, Arcavacata di Rende (Cs), Italy*
[b] *Department of Civil, Environmental and Architectural Engineering, University of Padova, via Loredan 20, 35131, Padova, Italy*

ARTICLE INFO

ABSTRACT

In October 2020, for the first time in its thousand-year-old history, the Venice Lagoon has been temporarily closed. The first operations of the Mo.S.E. system, a set of artificial barriers built to isolate the lagoon from the sea in case of high tides, prevented Venice and the other lagoonal settlements from flooding. Beyond its historical value, the closure of the lagoon inlets has led to unprecedented scenarios from a hydrodynamic standpoint. With the Mo.S.E. system operational, significant high tides can no longer be recorded within the lagoon and the undisturbed tide propagation can only be estimated through hydrodynamic modelling. When the inlets are closed and the effect of tide propagation nullified, the action of wind on cross-lagoon setup is enhanced and becomes more clearly recognizable, allowing for a robust calibration of the wind drag coefficient also for low to moderate wind speed. Furthermore, the data collected during the first closures of the Mo.S.E. gates allowed evaluating the real intra-gate infiltration entering the lagoon through the closed gates, and suggested that the gate operation produces some seaward disturbance as well.

1. Introduction

From the very beginning, Venice has endured by transforming the surrounding natural environment (Brambati et al., 2003). For more than a thousand years, Venetians carried out hydraulic works to preserve the strategic role of their lagoon for economic and safety purposes. They diverted large rivers out of the lagoon to avoid siltation, built large sea walls called Murazzi, modified the inlets, and dug new deep canals (D'Alpaos, 2010; Silvestri et al., 2018). The operation of the Mo.S.E. system stands for another step in the Venetian tradition of managing the lagoonal environment to enable the historical heritage of Venice and the related industrial and economic activities to survive.

In the last years, climate change and local geodynamics have progressively increased the flooding frequency in the Venice Lagoon (Lionello et al., 2012; Scarascia and Lionello, 2013; Mel et al., 2013), with a relative sea level rise marching at almost 6 mm per year (Mel et al., 2019a). In November 2019, the Venice Lagoon experienced a month of succeeding high tides that struck the whole basin, causing multiple devastating flooding (Cavaleri et al., 2020), leading some inhabitants to leave the city, and compromising tourism. Buildings, boats, and assets throughout the lagoon were ravished by the storms, with millions of

Euros worth of damage and widespread disruption.

A system of mobile barriers, known as the Experimental Electromechanical Module (Mo.S.E.), has been built since 2003, aimed at closing the lagoon inlets temporarily to protect Venice and the other urban settlements within the lagoon from flooding during high tide event exceeding a prescribed threshold. The Mo.S.E. system, a set of 78 independently oscillating gates, are meant to mitigate the effect of the increasing number of high tide events without threatening the lagoon ecosystem or affecting its landscape (Eprim et al., 2005; Trincardi et al., 2016).

On 3, 15 and 16 October 2020, for the first time ever, the Mo.S.E. system was operated during high tide conditions; the settlements within the lagoon remained dry, providing a great benefit for the local people. Beyond the actual testing stage, the completion of the whole Mo.S.E. system is expected by the end of 2021, with the raising of most of the pavements located in the lowest areas of the city of Venice to the safeguard threshold of 1.10 m (Ruol et al., 2020). These combined measures will allow protecting more than 90% of the municipal territory of Venice from flooding.

The construction and operation of a huge hydraulic infrastructure such as the Mo.S.E. system entails many open issues, including the

---

* Corresponding author.
E-mail addresses: riccardo_alvise.mel@unical.it (R.A. Mel), daniele.viero@unipd.it (D.P. Viero), luca.carniello@unipd.it (L. Carniello), andrea.defina@unipd.it (A. Defina), luigi.dalpaos@dicea.unipd.it (L. D'Alpaos).

vulnerability of the structures, changes in water renewal dynamics affecting the ecosystem, and long-term effects on the bio-morphodynamic evolution of the lagoon (Del Bello, 2019; D'Alpaos et al., 2011; Pivato et al., 2020; Viero et al., 2016; Umgiesser, 2020; Tognin et al., 2020, 2021).

The recent closures of the Mo.S.E. barriers gave us a chance to draw some hydrodynamic considerations on the behaviour of the temporarily closed/regulated Venice Lagoon that, for the first time, are based on real data and not on hypothetical scenarios (e.g. Umgiesser and Matticchio, 2006; Rinaldo et al., 2008; Mel et al., 2019a; Umgiesser, 2020; Mel et al., 2021).

In the present study, based on the analysis of recorded water levels in

and outside the lagoon and on the use of a hydrodynamic model, the focus is first on the detection and quantitative evaluation of the intra-gate infiltration, i.e., the flow rate that passes through the 78 gates composing the four Mo.S.E. barriers, which are not watertight as each gate is free to oscillate independently. Second, a robust estimation of wind drag coefficient for the Venice Lagoon is made to check the results by Mel et al. (2019a) and to complete the analysis by accounting for the effect of modest wind speeds; this is because the cross-lagoon setup is more clearly recognizable when the lagoon is temporarily closed, as it is no more disturbed by tide propagation. The calibrated hydrodynamic model is then applied to reproduce the actual storm events with the closure of the Mo.S.E. barriers, and then to simulate and analyze the
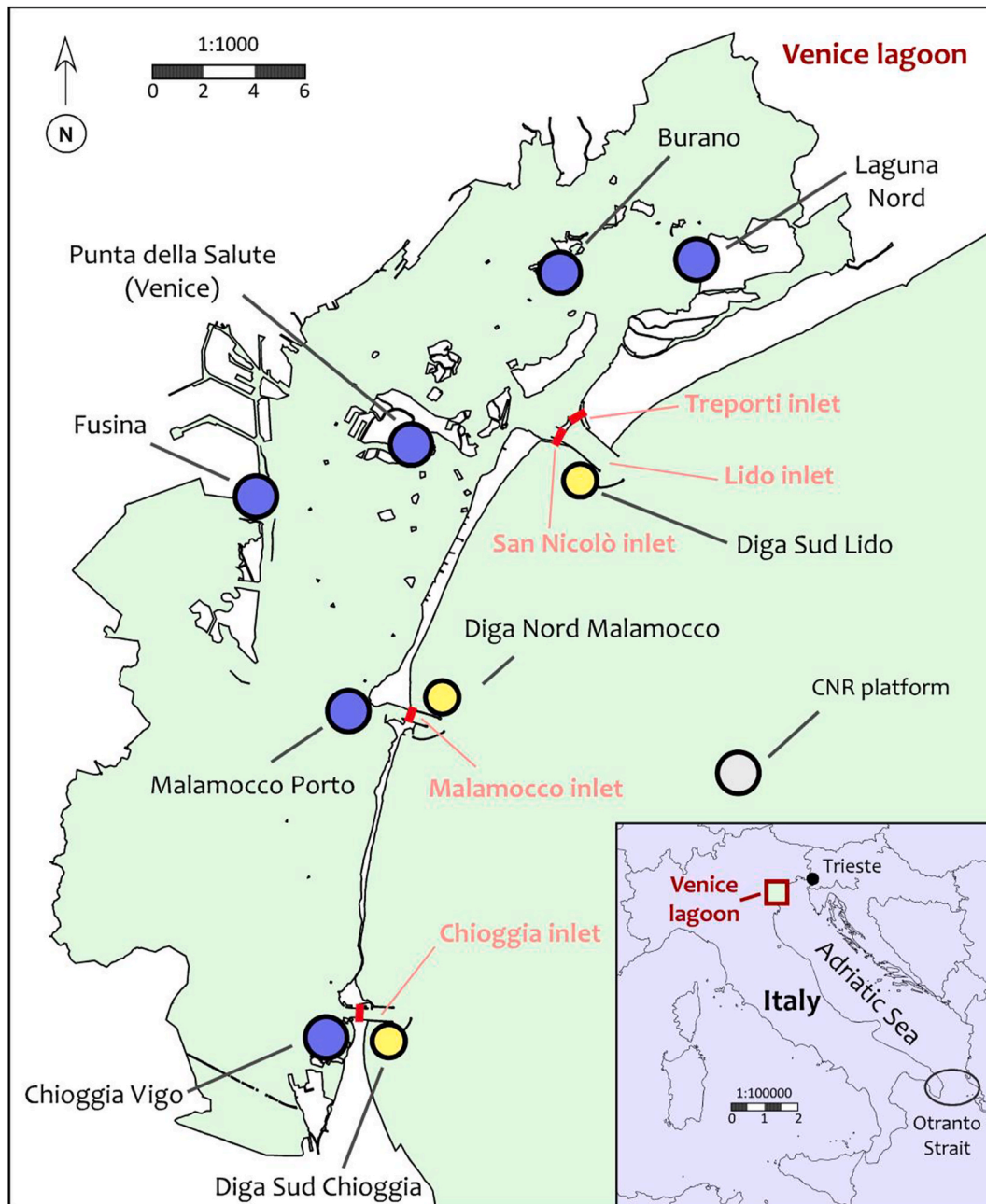
Fig. 1. The Venice Lagoon with the network of meteorological and tide stations used in the present work (tide forecasting and warning centre, CPSM): the lagoonal gauges of Chioggia Vigo, Malamocco Porto, Fusina, Punta della Salute, Burano and Laguna Nord (blue); Diga Sud Chioggia, Diga Nord Malamocco and Diga Sud Lido gauges, located seaward close to the inlets (yellow); CNR platform, located about 15 km in front of the Venice Lagoon (grey). Thick red lines show the location of the Mo.S.E. barriers. Data for the Trieste gauge has been provided by the Regional Civil Protection Office. (For interpretation of the references to colour in this figure legend, the reader is referred to the Web version of this article.)

associated "what if' scenarios that, this time and for the first time, refer to the undisturbed, non-regulated hydrodynamics of the Lagoon, i.e., with no Mo.S.E. operational. Finally, the water levels measured outside the Venice Lagoon during the first operations of the barriers show that the Mo.S.E. closure produces some sea level disturbance also outside the lagoon.

2. Materials and methods

2.1. The study area

The Venice Lagoon is located at the upper end of the Adriatic Sea, which is an elongated semi-enclosed basin connected with the Mediterranean Sea through the Otranto Strait (Fig. 1). The northern part of the Adriatic Sea is one of the Mediterranean regions most exposed to storm surges (Mel et al., 2014; Mel and Lionello, 2014; Rizzi et al., 2017; Ferrarin et al., 2020), because *i)* it has one of the highest tidal excursions in the Mediterranean Sea (about 1 m at spring tide), *ii)* the water setup, triggered by the so-called Sirocco wind that blows from South-East almost parallel to the Adriatic main axis, is enhanced by the local orography, the shallow water depth, and by small-scale processes (Marcos et al., 2009; Pasaric et al., 2009; Ruol et al., 2018), and *iii)* once a storm is over, a seiche forms which keeps the basin oscillating for few days with fundamental periods of about 11 and 22 h (Cerovečki et al., 1997; Lionello et al., 2005). Hence, the magnitude of storm surge in the northern Adriatic Sea, as well as the flooding probability of Venice and other exposed settlements, depend on the relative phase of these different forcings.

The Venice Lagoon is a shallow coastal transitional water body connected to the Adriatic Sea by four inlets, from north to south: Treporti, San Nicolò, Malamocco, and Chioggia (note that the northern inlet, formerly the "Lido" inlet, has been divided in two parts, namely "Treporti" and "San Nicolò", by the Mo.S.E. infrastructure, see Fig. 1). The Lagoon is a very complex natural and anthropic system, consisting of an extensive network of natural and artificial channels, tidal flats, salt marshes, and a number of small inhabited islands (Carniello et al., 2009). The historical city of Venice is located quite close to the San Nicolò inlet (Fig. 1).

Flooding from even modest tides and storm surges is an increasingly frequent threat for the historical and cultural heritage of the Venice Lagoon, for tourism, and for economic activity as well. Several urban settlements located within the Venice Lagoon, in fact, have the pavement level set at about 1.2 m above the official reference datum on average, and even lower in the most prominent parts (e.g., St. Mark's square, Rialto Bridge vicinity, and most of the Burano streets are at about 0.9 m). Flooding frequency is increasing due to the combined effect of sea level (SL) rise, land subsidence, and climate change (Brambati et al., 2003; Rinaldo et al., 2008; Carbognin et al., 2010; IPCC, 2013; Reimann et al., 2018; Molinaroli et al., 2019).

As an important note, when expressing elevations, in the present work we refer to the official mareographic reference of Punta della Salute (PS) gauge, located in the city centre of Venice (Fig. 1), whose datum corresponds to the mean SL recorded during the 1885–1909 period. This datum is 23 cm below the national datum, named IGM1942 (Comune di Venezia, 2020). The mareographic reference of Punta della Salute is generally used as the practical reference to indicate which parts of the urban settlements of the lagoon are flooded for a given SL (Cavaleri et al., 2020). At present, based on observed data in the period 2010–2019, the PS datum is located 34 cm below the mean SL.

2.2. The Mo.S.E. system and the safeguard threshold

The Mo.S.E. system was designed in 1984, it is under construction since 2003 by the *Ministry of Infrastructure and Transport - Provveditorato Interregionale per le Opere Pubbliche del Triveneto* and it is supposed to be completed by the end of 2021. The Mo.S.E. system is conceived to protect the Venice Lagoon by isolating the lagoon from the sea by means of an integrated system of four separate flood barriers crossing the inlets (Fig. 2). Each barrier consists of some individual steel flap gates 20 m wide, 5 m thick, and between 18 and 28 m high. 21 gates constitute the barrier of Treporti, 20 the barrier of San Nicolò, 19 the barrier of Malamocco, and 18 the barrier of Chioggia (see https://www.mosevenezia.eu/progetto/ for more technical details). In ordinary tidal conditions, the gates are filled with water, resting on their housing caissons located at the bottom of the inlets. To raise the gates and close the lagoon inlets, compressed air is introduced into the gates, which are connected to the concrete foundation through steel hinges (Bertagnoli et al., 2017). The barriers are designed to disconnect the lagoon from the sea for SL up to 3 m, and are expected to remain raised for all the duration of a flood event. Then, the gates are refilled with water and sink down. The system is equipped with navigational locks to allow port activities during closure events (Cavallaro et al., 2017).

Following the flood event of 12 November 2019, in which the SL reached 1.87 m, the Italian Government accelerated the works to complete the construction of the Mo.S.E. system. On 10 July 2020, the four barriers have been tested for the first time, in fair weather conditions. The Mo.S.E. system was then ready to protect the lagoon settlements from the high tides that typically occur in Autumn.

The goal of the Mo.S.E. system is to limit the SL below prescribed safeguard thresholds. The safeguard threshold is set at 1.10 m for Venice, Murano, and Burano, and at 1.30 m for Chioggia (southern lagoon, Fig. 1), which is protected by a second local system of movable barriers (Eprim et al., 2005; Mel et al., 2019a, 2021; Umgiesser et al., 2020).

2.3. The storm events that led to the first Mo.S.E. operations in October 2020

During the ongoing testing phase of the Mo.S.E. system, which lasts from June 2020 to December 2021, the barriers are planned to close when the forecasted SL exceeds the threshold value of 1.30 m at PS or Chioggia. This condition occurred in the mornings of 3, 15, and 16 October 2020. The three storm events that caused the first operations of the Mo.S.E. system in October 2020 are briefly described in the following sections (details on the meteorological scenarios can be found in the Supplementary Material).

2.3.1. The storm event of 3 October 2020

Since the last days of September 2020, the wind setup, combined with the reverse baric effect (i.e., atmospheric pressure higher in the southern Adriatic Sea and lower in its northern part) increased the SL in the northern Adriatic Sea and led to several occurrences of SL ≥ 0.80 m at PS, which is the yellow risk code as defined by the tide forecasting and warning centre (CPSM). The strongest wind speed in the northern Adriatic Sea occurred on 3 October morning, reaching peak values of 14 m/s around 9:00 CET at the CNR platform gauge (Fig. 3c).

The SLs of the 3 October storm event were predicted well by the oceanographic models with a lead time of several days. With a surge residual of about 0.6 m (which is not exceptionally high, see Mel et al., 2014), superposed to the astronomical tide, the SL peak in the Venice Lagoon was predicted to slightly exceed 1.30 m in the late morning of 3 October. During the real storm event, consistently with the forecast, the CPSM gauges located seaward of the inlets (yellow bullets in Fig. 1) recorded SLs above the safeguard threshold of 1.10 m for about 4 h (Fig. 3a). The SL peak recorded at Diga Sud Lido was 1.32 m; slightly lower values were measured at Diga Nord Malamocco (1.27 m) and Diga Sud Chioggia (1.23 m), with a SL gradient along the Venetian coast caused by the Sirocco wind (Fig. 3a).

The Mo.S.E. barriers started raising at 7:30 CET, gradually reducing the flow from the sea to the lagoon, until 8:50 CET, when all the gates reached the elevation of 3 m. The closure of the inlets limited the SL at the PS gauge to 0.77 m, which rapidly dropped to 0.70 m due to the propagation of the tidal wave within the lagoon. At Chioggia Vigo,
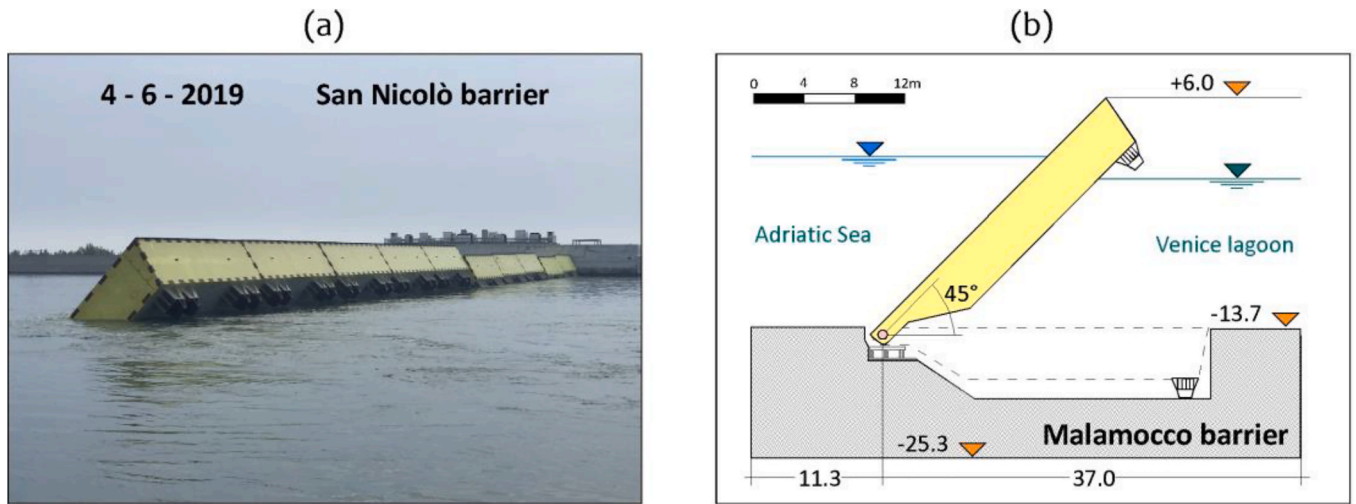
Fig. 2. Mo.S.E. system. (a) view of the flap gates of the San Nicolò barrier partially raised under the test of 4 June 2020 (photo by R.A. Mel); (b) working position of a single flap gate of the Malamocco barrier (data in meters and elevations referred to the PS reference datum).
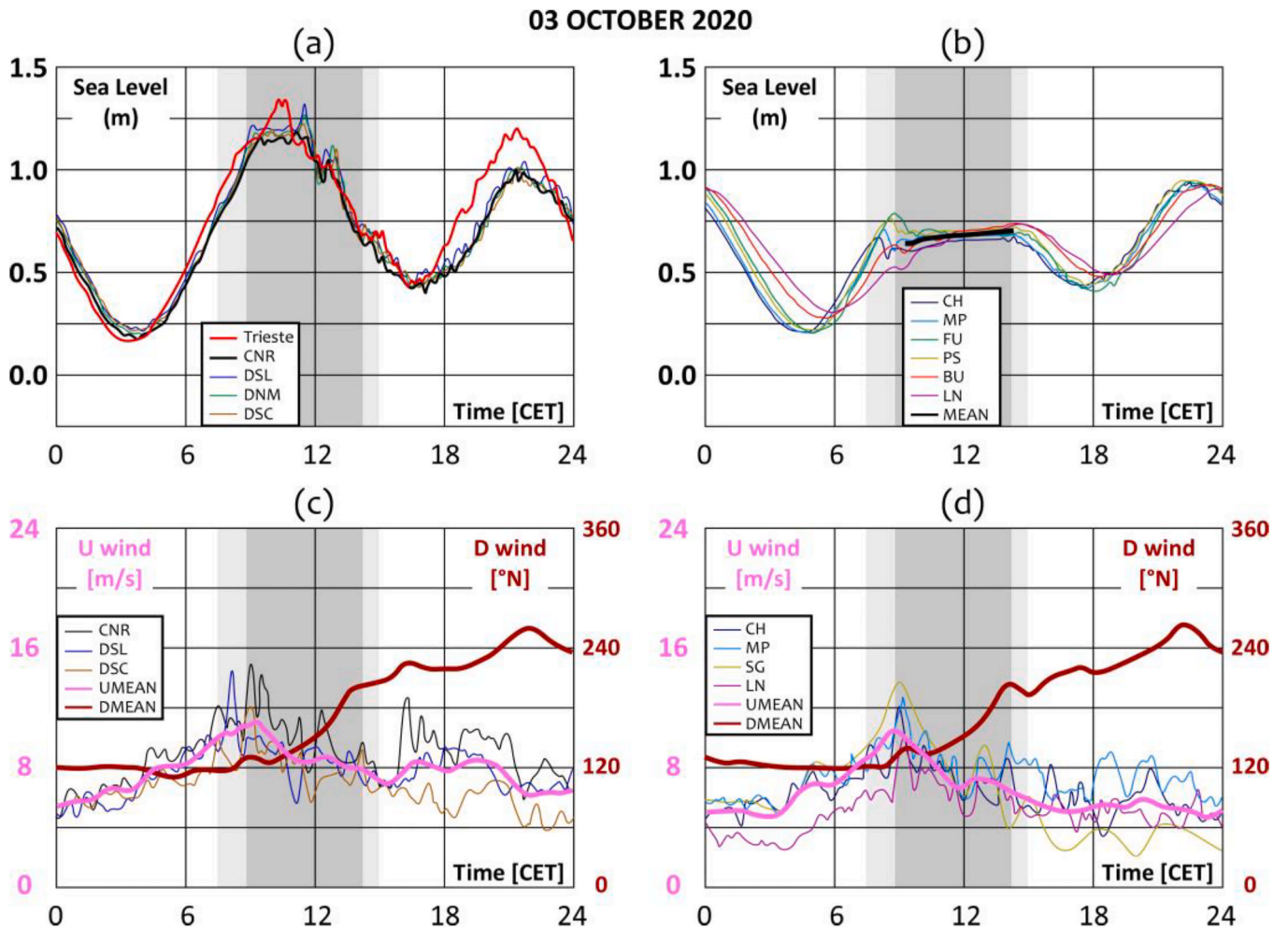

Fig. 3. Storm event of 3 October 2020. Grey shaded areas denote the closure period (the light grey areas denote the raising and lowering phases). (a) Observed SLs at the seaward gauges of the Venice Lagoon and at Trieste; (b) observed SLs at the six lagoonal gauges (the black thick line is the average of the six values filtered by an hourly moving average); (c) observed wind speed at the seaward gauges (Diga Sud Chioggia, Diga Sud Lido and CNR platform) and (d) at the lagoonal gauges (Chioggia Porto that is close to Chioggia Vigo, Malamocco Porto, San Giorgio that is located in the city centre of Venice, and Laguna Nord). The average wind speed (pink thick lines) and the average wind direction (dark red thick lines) are also reported. (For interpretation of the references to colour in this figure legend, the reader is referred to the Web version of this article.)

located in the southern lagoon, hereinafter named Chioggia, the SL peak stopped at 0.68 m, due to the negative wind setup in the windward part of the lagoon induced by the Sirocco wind. The SL difference between Diga Sud Lido (outside the lagoon) and PS reached a maximum of about 0.6 m at 11:30 CET. Similar SL differences were measured in the southern lagoon (0.55 m between Diga Sud Chioggia and Chioggia). The gates started sinking at 14:10 CET, when the decreasing SL outside the inlets reached values comparable to the SL within the lagoon.

During the closure of the barriers, a gradual increase of the SL at the six CPSM lagoonal gauges (blue bullets in Fig. 1) clearly appears in the SL records. After filtering these SL data through an hourly moving average and then computing the mean value of the six gauged values (black thick line in Fig. 3b), we obtain that the mean SL increased from 0.64 m at 9:20 CET (i.e., half an hour after the complete closure of the barriers, when the main SL oscillations within the lagoon are mostly dissipated), to 0.70 m at 14:20 CET.

As a final note, the irregular trend of SLs observed at the sea gauges (Diga Sud Lido, Diga Nord Malamocco, Diga Sud Chioggia located at the Venice Lagoon inlets, CNR platform, and Trieste, see Fig. 1) just after the closing of the Mo.S.E. barriers suggests that some minor hydrodynamic disturbance have been produced outside the gates and in the Northern Adriatic Sea between the Venetian coast and the Trieste Gulf (Fig. 3a). This aspect is analyzed in Section 3.3.4.

2.3.2. The storm event of 15–16 October 2020

The meteorological scenario of 13–16 October 2020, well forecasted by meteorological and oceanographic models, resulted in an estimated surge residual of about 0.5 m for 15 October, and 0.40–0.45 m for the morning of 16 October, mostly caused by the 22-h Adriatic seiche triggered by the surge of 15 October. Although both surges were lower than that occurred on 3 October, the peaks of surge residual almost coincided with the morning spring tidal peaks on 15 October (0.81 m) and on 16 October (0.84 m, at the new moon day). The combination of astronomical and meteorological contributions led to an overall SL forecast of 1.35 m on 15 October and of 1.25–1.30 m on 16 October (data from the CPSM forecasting center).

Consistently with these forecasts, the seaward gauges recorded SLs above the safeguard threshold for Venice (1.10 m) for about 3.5 h during the morning of 15 October and for about 2 h on 16 October. On 15 October, Diga Sud Lido recorded 1.35 m, while higher SL values were recorded at Diga Nord Malamocco and Diga Sud Chioggia (1.40 m and 1.44 m respectively), with a SL gradient along the Venetian coast caused by the Bora wind (Fig. 4a).

On 15 October, the Mo.S.E. barriers were raised from 6:10 CET to 7:10 CET, when all the gates were 3 m above the local datum. The closure of the inlets limited the SL at the PS gauge to 0.65 m, which rapidly dropped to 0.47 m due to the tide propagation and the wind setup induced by the local Bora wind field. At Chioggia, in the southern lagoon, the SL reached 0.92 m, with a SL difference between Chioggia and PS greater than 0.40 m, due to the wind setup effect. The maximum SL difference between Diga Sud Lido (outside the lagoon) and PS reached about 0.90 m at 9:00 CET, while in the southern lagoon the SL difference between Diga Sud Chioggia and Chioggia was almost 0.60 m. The barriers started dropping shortly after 12 CET, beginning from the
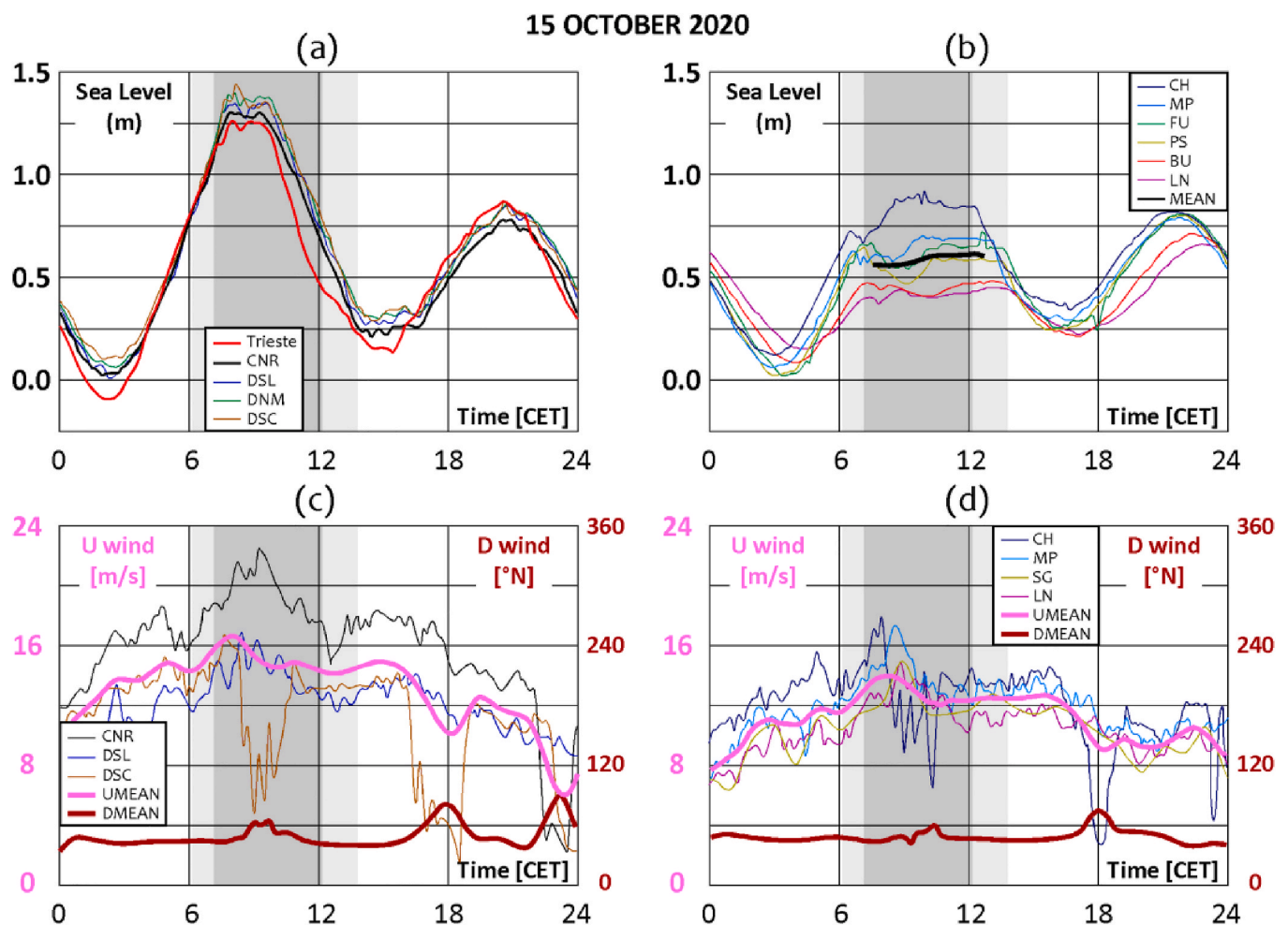

Fig. 4. Storm event of 15 October 2020. (a) Observed SLs at the seaward gauges and at Trieste; (b) observed SLs at the six lagoonal gauges. Observed wind speeds and direction at the seaward gauges (c) and at the lagoonal gauges (d). See the caption of Fig. 3 for additional details.

Chioggia inlet where the decreasing outer SL matched the lagoon SL before than at the other inlets, due to the wind setup.

On 16 October, the SLs gauged at the seaward gauges were just under 1.20 m (1.17 m at Diga Sud Lido and Diga Sud Chioggia, and 1.16 m at Diga Nord Malamocco). The Mo.S.E. barriers raised from 6:10 CET to 7:10 CET, settling the SLs to about 0.45 m at PS and to 0.50 m at Chioggia with a maximum SL difference between the sea and the lagoon of almost 0.75 m. The barriers started dropping at 12:30CET.

Both events showed an increase of the mean lagoonal SL during the closure phase, almost 0.04 m on 15 October and about 0.05 m on 16 October (Figs. 4b and 5b), and, again, anomalous SL oscillations were measured at the seaward gauges (Figs. 4a and 5a).

2.4. The WWTM hydrodynamic model

We analyzed the hydrodynamic flow field triggered by the wind-wave, climate, and tidal forcing, with and without the closure of the Mo.S.E. barriers, using the WWTM two-dimensional mathematical model (Carniello et al., 2005, 2011). WWTM is a coupled wind wave-tide model that solves the full shallow water equations on unstructured grids through a finite element, mixed Eulerian-Lagrangian, numerical scheme based on the Galerkin's approach (D'Alpaos and Defina, 1993; Defina, 2003; Martini et al., 2004; D'Alpaos and Defina, 2007; Viero et al., 2013). The hydrodynamic module solves the 2D shallow water equations modified to deal with wetting and drying efficiently using the physics-based approach by Defina (2000). The wind-wave module solves the wave action conservation equation,

parameterized using the zero-order moment of the wave action spectrum in the frequency domain. In the last two decades, the WWTM model has been extensively tested in Venice Lagoon and in other shallow coastal and transitional water bodies (e.g., Carniello et al., 2005; D'Alpaos and Defina, 2007; Mariotti et al., 2010; Zarzuelo et al., 2018). Recently, it has been used to reproduce the effect of the temporary closure of the Venice Lagoon inlets through the raising of the movable gates of the Mo.S.E. system (Mel et al., 2019a, b).

The computational mesh used in this study, which includes the Venice Lagoon and a portion of the northern Adriatic Sea for a total area of approximately 10,000 km^2, is made of about 150,000 triangular elements and 80,000 nodes. The representative size (side-length) of the elements is about 1000 m in the Adriatic Sea and 100 m in the Venice Lagoon, whereas the smallest size is about 10 m at the lagoon inlets, where the spatial gradients of the velocity are larger. This model of the Venice Lagoon has been calibrated and verified in previous studies (Carniello et al., 2005, 2011, 2011; Matticchio et al., 2017) by comparing the model results with measures of SLs, discharges through the inlets and major tidal channels, and local water velocity from drifting buoys trajectories.

In the present work, for analysing the three storm events, we focused the analysis on the lagoon hydrodynamics. The model is forced by imposing the gauged SL seaward just outside the three inlets (i.e., Diga Sud Lido, Diga Nord Malamocco, and Diga Sud Chioggia) and by reconstructing the spatial and temporal distribution of the wind field according to Carniello et al. (2012) based on anemometric data collected at the Laguna Nord and Chioggia Porto gauges (northern and southern
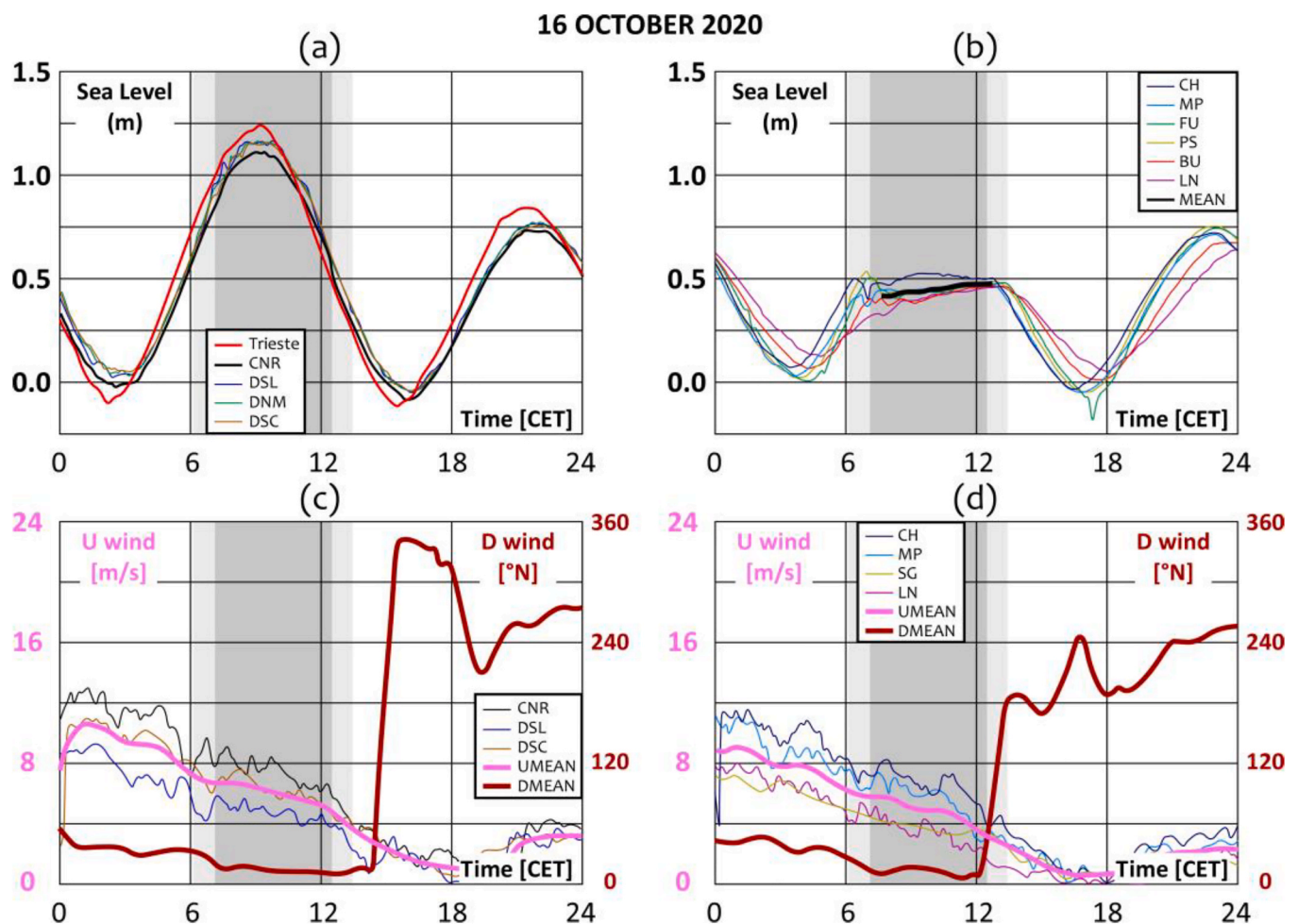

Fig. 5. Storm event of 16 October 2020. (a) Observed SLs at the seaward gauges and at Trieste; (b) observed SLs at the six lagoonal gauges. Observed wind speeds and direction at the seaward gauges (c) and at the lagoonal gauges (d). See the caption of Fig. 3 for additional details.

part of the lagoon, respectively, see Fig. 1). The wind shear stress at the water surface, τ_{WIND}, is computed as

$$\tau_{WIND} = \rho_a C_D U_{WIND}^2 \qquad (1)$$

where ρ_a is the air density, U_{WIND} is the wind speed at 10 m, and C_D is the drag coefficient, subject to a dedicated calibration procedure as described in Section 3.2.

3. Results and discussion

3.1. Estimation of the intra-gate infiltration rate

The SLs measured within the lagoon during the closing phase of the Mo.S.E. barriers showed an average increase, which is due to the rainfall height within the lagoon and to the hydrological runoff from the ~2000 km² mainland area contributing to the lagoon, as well as to the run-through discharges through the Mo.S.E. barriers. Indeed, the 78 gates composing the barriers are free to oscillate and not connected one to each other, which means that the barrier is not watertight; the width of the open passages between the gates can temporarily increase when the gates oscillate due to sea waves (Pirazzoli, 2002; Rinaldo et al., 2008; Umgiesser and Matticchio, 2006). According to experiments carried out on a large physical model at scale 1:10 (Consorzio Venezia Nuova, 2003, 2006), this intra-gate infiltration depends on the SLs gradients, the gap between the gates and their angle of oscillation.

The SL data gauged during the storm events of October 2020 allowed for a first quantitative assessment of the flow rate entering the lagoon through the inlets during the closure of the barriers, due to the intra-gate infiltration. The duration of the three closures, i.e., when the gates are above the mean SL, was about 5h 50'. The increase in SL within the lagoon was estimated by analysing the average SL at the six lagoonal gauges, filtered through an hourly moving average. Estimating the contribution of freshwater runoff to the Venice lagoon is quite a difficult task, being the result of a complex interrelation between natural and anthropogenic processes. Rinaldo et al. (2008) showed that the volume discharged into the lagoon from the watershed is about 9% of the rain directly falling over the lagoon. Accordingly, for the considered events, we used the rainfall time series to estimate the contribution to SL increase ascribed to direct rainfall and to hydrological runoff, which came out to be less than 10% with respect to the observed mean lagoonal level increase. By aggregating the data of the three events, in fact, we found an average SL (blue line in Fig. 6a) increasing at a rate of about 10 mm/h; after subtracting the direct rainfall and hydrological runoff (green line in Fig. 6a), we found the SL increasing at an average rate of

about 9 mm/h due to intra-gate infiltration (red line in Fig. 6a). Such a value falls within the plausible range referred to in the study by the International College of Experts (1998). In that study, the SL increasing rate due to intra-gate infiltration was estimated in 2.7 mm/h assuming no gate oscillation, in 4.5 mm/h with gate oscillations due to low-–moderate waves, and up to 21 mm/h in case of strong oscillations due to storm waves.

The total discharge due to intra-gate infiltration can be estimated using a classical formulation for orifice flow as

$$Q_{in} = C_Q \sqrt{2g\Delta h} \qquad (2)$$

where C_Q is a discharge coefficient, g is gravity, and Δh is the SL difference across the gates. Considering that the discharge coefficient depends on cross-sectional area and flow contraction, which are both expected to vary according to the gate oscillation and the presence of waves, the value of C_Q was calibrated to match the observed SL increase due to intra-gate infiltration in the three considered events. We obtained $C_Q = 266 \text{ m}^2$, which corresponds to a cross-sectional flow area of about 200 m² (the sum of intra-gate gaps multiplied by the water depth) multiplied by a factor of 1.33; this large value confirms that the effective intra-gate area is indeed affected by the gate oscillation. Eq. (2) was further validated on the data collected during the event occurred on 4–6 December 2020 (see Figure S.5 in the Supplementary Material), when the Mo.S.E. barriers were closed for almost 48 h, predicting the variation of the mean lagoonal SL with an accuracy of ~2%.

For the three events, the discharge entering the Venice Lagoon due to intra-gate infiltration, computed with Eq. (2), is up to 1000 m³/s (Fig. 6b). In the numerical simulations, we distributed such a contribution among the inlets as a function of the barrier frontal area: 16% for Treporti, 29% for San Nicolò, 31% for Malamocco, and 24% for Chioggia. The average effect on the SL increase within the lagoon, estimated by the WWTM model using this approach, is shown by the red dashed line in Fig. 6a.

3.2. Calibration of the wind drag coefficient for the Venice Lagoon

3.2.1. Why the need of calibrating the drag coefficient?

A wealth of experimental and numerical studies is available in the literature that deal with the processes occurring at the sea-air interface. It has been highlighted that the wind drag coefficient, C_D, strongly depends on the sea roughness, which in turn depends on the characteristics of waves (height, shape, and steepness, which depend on wind speed, fetch, wave age, water depth, etc.), on the (mis)alignment between wave and wind direction, on non-stationarity of submeso winds, etc.
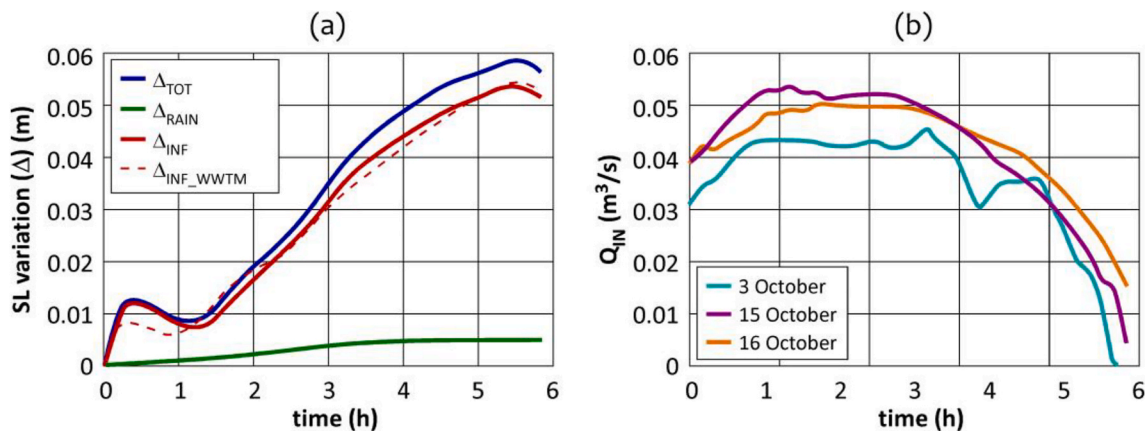

Fig. 6. (a) Time variation of the mean SL measured within the Lagoon during the gate closures, using aggregated data of the three closures of October 2020. Total SL increase (Δ_{TOT}, blue line), contribution due to direct rainfall and hydrological runoff (Δ_{RAIN}, green line), and the net contribution of the intra-gate infiltration (Δ_{INF}, red line). The red dashed line (Δ_{INF_MOD}) is the SL increase computed by WWTM using Eq. (2) to compute the intra-gate infiltration, shown in panel (b). (For interpretation of the references to colour in this figure legend, the reader is referred to the Web version of this article.)

(Charnock, 1955; Edson et al., 2013; Mahrt et al., 2016; Porchetta et al., 2019; Smith et al., 1992; Vickers and Mahrt, 1997). As a consequence of this complexity, very different formulations for C_D can be found in the literature (Bryant and Akbar, 2016; Sterl, 2017).

While it is generally valid that the sea surface is rougher for increasingly higher winds, for the specific case studied herein it is worth recalling that, over shallow waters, the roughness of the surface is higher than that in open ocean for corresponding values of wind speed (see Bi et al., 2015; Jiménez and Dudhia, 2018; Shabani et al., 2014; Zhao et al., 2015). Moreover, it is well-known that young waves are rougher than older ones (Donelan, 1982; Janssen, 1989; Smith et al., 1992; Porchetta et al., 2019), and the limited fetch in semi-enclosed tidal basins limits the presence of old waves in favour of young ones, with higher peak frequency (Carniello et al., 2011; Fagherazzi and Wiberg, 2009; Vickers and Mahrt, 1997). Pareja-Roman et al. (2019), studying a shallow coastal plain estuary in Delaware Bay, found that the spatial distribution of wave height and age is controlled by bathymetry and fetch; this has implications for the drag coefficient in young, underdeveloped seas, which is found to be up to 30% larger with respect to parameterizations in which surface drag is only a function of wind speed. Shabani et al. (2014) reported drag coefficients in the surf zone of twice the values as for open ocean conditions. Ortiz-Suslow et al. (2015), studying a river inlet in North Carolina to evaluate wind stress parameterizations in coastal areas, concluded that open ocean parameterizations underestimate the drag coefficient by a factor of 2.6. According to Ortiz-Suslow et al. (2018), while the drag coefficient is typically well predicted in open sea, the influence of depth-limited processes on drag still remains underexplored; they found that, on average, the parameterized values underestimate the drag by O(2–4) times, although there was a considerable spread (generally ±100%) about these means. Kim et al. (2019) showed that meteorological models typically overestimate the wind speed over regions of shallow waters when the effects of water shallowness are not accounted for properly.

From the above picture, it follows that for the Venice Lagoon, which is a semi-enclosed tidal basin with an elongated shape, relatively shallow waters, and large portions characterized by a complex morphology with emerging islands and salt marshes, the wind drag coefficient needs to be properly calibrated to model the cross-lagoon wind setup accurately.

3.2.2. Calibration of the wind drag coefficient

During the closure of the Mo.S.E. barriers, tidal propagation is nullified within the Venice Lagoon and the action of wind becomes by far the most important factor that redistributes the water mass within the basin, leading to a SL increase downwind and to a simultaneous SL decrease upwind (Zecchetto et al., 1997; Carniello et al., 2011; Mel et al., 2019b; Umgiesser, 2020). Furthermore, the wind setup within the temporarily closed lagoon is expected to be larger than in the non-regulated scenario, for which the fluxes through the three inlets can naturally adjust to level out the inner SL gradient (Mel et al., 2019a). All these aspects suggest that the operations of the Mo.S.E. barriers are a favourable opportunity to assess the hydrodynamic effects of local winds blowing over the Venice Lagoon.

In the previous studies by Mel et al. (2017, 2019b), the wind drag model in WWTM (hereinafter referred to as *Mel2017*) was calibrated by simulating storm events in the period 2000–2012, characterized by wind speeds greater than 12 m/s. The calibration procedure did not include moderate winds (say $U_{WIND} < 12$ m/s) that, in the non-regulated scenario, produced wind setups that were largely masked by the effects of tide propagation. They found a quasi-linear dependence of C_D on the wind speed, with a null intercept.

In the present study, the analysis of the wind setup recorded during the three events of October 2020, when the Mo.S.E. barriers were closed, allowed for a thorough calibration of the wind drag coefficient, C_D, considering wind speeds lower than 12–15 m/s. To complete the analysis, we considered four additional historical storm events, for which the

Mo.S.E. was not operational, characterized by winds blowing for a sufficiently long time with an almost constant speed and direction, and by different tidal and meteorological conditions (see Table 1 and Figure S.4 in the Supplementary Material for additional details). The calibration set then consisted of seven storm events on the whole.

The wind setup was evaluated as the SL difference (hereinafter noted as ΔSL) between PS and Chioggia; indeed, the regular morphology of the basin between PS and Chioggia does not play a significant role on the dynamics of the water mass and the wind setup becomes more clearly recognizable. The calibration period in which the ΔSLs obtained using WWTM were compared with measured data was chosen according to these criteria: (a) inlets closed for at least 1 h (for dissipating residual tide propagation) and $U_{WIND} > 5$ m/s for events with the Mo.S.E. operational, and (b) $U_{WIND} > 15$ m/s for unregulated events.

For the sake of simplicity, we assumed a linear relationship of C_D with the wind speed in the form

$$C_D = (C_{D0} + e_W \cdot U_{WIND}) \cdot 10^{-3} \tag{3}$$

and relaxed the hypothesis of null intercept previously assumed by Mel et al. (2017), as it is not supported by the physics of the problem (Chen et al., 2019; Edson et al., 2013; Smith, 1980; Vickers and Mahrt, 1997).

To obtain an optimal estimate of C_{D0} and e_W, we simulated with WWTM the seven storm events selected for calibration using different values of C_{D0} in the range 0.49–0.61, i.e., from the value proposed by Large and Pond (1981) to that by Smith and Banke (1975) and Smith (1980), and of e_W in the range 0.063–0.12, i.e., greater than the value proposed by Smith (1980). For each tested pair (C_{D0}, e_W) in the above ranges, we computed the mean error and the absolute root mean square error (RMSE) on ΔSLs, over the calibration periods, as well as on the peaks of ΔSL obtained through a 1 h moving average filtering, obtaining similar results. We finally chose the best-fit pair looking at peak values, assuming that the peak values of ΔSL are less disturbed by uncertainties in the spatial and temporal distribution of the wind field.

As the best-fit wind drag model for the Venice Lagoon, hereinafter denoted as *Mel2020*, we found $C_{D0} = 0.61$ and $e_W = 0.085$ s/m, corresponding to a RMSE of 0.014 m, an almost zero mean error, and a maximum error of 0.025 m on the calibration events. For the sake of comparison, we note that the operational model for storm surge forecasting in the Venice Lagoon (Bajo et al., 2007; Bajo and Umgiesser, 2010) uses the original formulation proposed by Smith and Banke (1975), which adopts the same C_{D0} of *Mel2020* and a similar, yet 12% lower, e_W coefficient.

Fig. 7a shows the drag formulation by *Mel2020* (green), *SB1975* (Smith and Banke 1975, black dashed line), *Sm1980* (Smith, 1980, grey dashed line), *Mel2017* (blue), and *LP1981* (Large and Pond, 1981, purple). In the figure, the dots locate the seven calibration events according to the average (circles) and maximum (diamonds) wind speeds and ΔSLs, and the associated C_D computed with Eq. (3) using the pair (C_{D0}, e_W) that performed best for each specific storm event; such a visualization shows the suitability of the different wind formulations for the Venice Lagoon.

Fig. 7b compares the modelled and measured data of ΔSL between PS and Chioggia using different wind drag formulations (binned data from the seven calibration events). *Mel2020* almost coincides with the 1:1 black line; *Mel2017* underestimates the setup by ~5% (as for *SB1975*, not shown in the figure); *LP1981* and *Sm1980* (not shown), which are typical formulations for open sea, lead to a larger (~15%) underestimation of the wind setup. The results obtained by neglecting the effect of wind (yellow line) are also reported in Fig. 7b for the sake of comparison.

Detailed data for the seven calibration events and for different drag formulations are reported in Table 1 and in Figure S.4 of the Supplementary Material. Remarkably, the maximum errors in the wind setup obtained using the *Mel2020* formulation are comparable to the measurement precision of the SL gauges.

Table 1
Calibration events. Data are computed within the calibration range. Measured data were previously filtered with an hourly moving average. In events 5*,6*, and 7*, the lagoon was temporarily closed by the Mo.S.E. system.

ID	Date	Mean wind direction	Mean wind speed	Max wind speed	Max ΔSL observed	Max ΔSL Mel2020	Max ΔSL Mel2017	Max ΔSL LP1981
1	**November 06, 2000**	140° N	17 m/s	18 m/s	0.30 m	**0.27 m**	0.25 m	0.23 m
2	**November 10, 2004**	30° N	17 m/s	18 m/s	0.33 m	**0.32 m**	0.29 m	0.26 m
3	**December 26, 2008**	60° N	17 m/s	18 m/s	0.23 m	**0.24 m**	0.23 m	0.21 m
4	**November 13, 2017**	30° N	20 m/s	23 m/s	0.46 m	**0.48 m**	0.47 m	0.41 m
5*	**October 03, 2020**	160° N	8 m/s	9 m/s	0.08 m	**0.07 m**	0.05 m	0.06 m
6*	**October 15, 2020**	50° N	14 m/s	16 m/s	0.40 m	**0.41 m**	0.37 m	0.34 m
7*	**October 16, 2020**	15° N	6 m/s	7 m/s	0.09 m	**0.09 m**	0.07 m	0.08 m
	Mean error					**0.000 m**	−0.023 m	−0.043 m
	RMSE					**0.014 m**	0.030 m	0.049 m
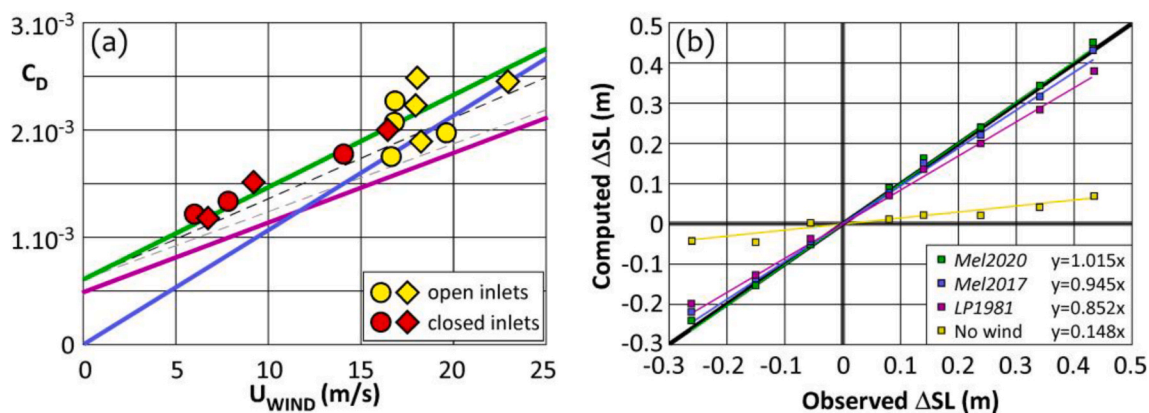
Fig. 7. (a) Calibration of the wind drag coefficient: *Mel2020* (green line), *Mel2017* (blue line), *LP1981* (purple line), *SB1975* (black dashed line), *Sm1980* (grey dashed line) formulations for C_D. Dots locate the seven storm events used for calibration (circles refer to average values for the whole calibration periods, diamonds to peaks only), with open (yellow) and closed (red) Mo.S.E. barriers. (b) Binned data of *ΔSL* between PS and Chioggia for the seven calibration events using different wind drag formulations. (For interpretation of the references to colour in this figure legend, the reader is referred to the Web version of this article.)

The need of using larger drag coefficients in the Venice Lagoon than in the open sea is neither new nor unexpected. Interestingly, in the first application of the SHYFEM model to the Venice Lagoon, Umgiesser et al. (2004) used a constant C_D equal to $1.5 \cdot 10^{-3}$, whereas in the following applications C_D was given larger values: Zampato et al. (2007) assumed a constant value of $2.5 \cdot 10^{-3}$; Bajo et al. (2007) and Bajo and Umgiesser (2010) adopted the formulation by Smith and Banke (1975), which gives larger values than the open-sea correction proposed by Smith (1980).

3.2.3. A remark on the use of a linear formulation for the drag coefficient

In the present study, the wind drag coefficient, C_D, has been calibrated in the reliable range of wind speed for the Venice Lagoon, i.e., $U_{WIND} < 24$ m/s. It is worth stressing that the linear relation here employed is not meant to be extrapolated to higher wind conditions. Indeed, for higher wind speeds, the effective surface roughness is lower than that given by the waves because wave breaking occurs and a layer of droplets and foam shields the waves from the wind; accordingly, for increasing wind speed, the drag coefficient has somewhere a maximum and then a decrease (Donelan et al., 2004; Sterl, 2017; Zhao and Li, 2019). The wind speed corresponding to the peak of C_D has been determined in about 30 m/s (Sterl, 2017), but this value may be lower in shallow waters as in the Venice Lagoon.

*3.3. Ex-post analysis of the Mo.S.E. closure events*

The three events of October 2020, during which the Mo.S.E. barriers were closed for the first time (Section 2.3), have been the subject of an ex-post analysis based on the calibrated WWTM hydrodynamic model. Interesting aspects, emerged from this analysis, are described in the following sub-sections.

3.3.1. "Natural" scenarios have become the "what if" scenarios

As hydrodynamic modelers, we are used to calibrate models on real "natural" events, and then to simulate hypothetical "what if" scenarios. In the Venice Lagoon, the "what if" scenario of the last two decades was that with the operation of the Mo.S.E. barriers. Now that the Mo.S.E. is operational, the "natural" hydrodynamic behavior of the Venice Lagoon has become the "what if" scenario.

With the Mo.S.E. barriers operational, high SLs are destined to disappear from the SL time series recorded within the Venice Lagoon, cut down by the temporary closure of the inlets; the SL peaks that would have occurred within the lagoon without the Mo.S.E. barriers, can now be estimated using modelling tools only. This is an important exercise; first, to assess the real contribution of the Mo.S.E. system to reduce SLs within the lagoon for protecting the urban area from flooding; second, to reconstruct and keep a complete time series of "undisturbed" SLs within the lagoon. This second point is useful, for example, to compute the exceeding probability for SL thresholds within the lagoon in the hypothetical scenario with no Mo.S.E., and even more to keep up-to-date the calibration of statistical models that are currently used to predict the surge inside the lagoon starting from the surge predicted in the North Adriatic (Bajo and Umgiesser, 2010). It has to be stressed, in fact, that the closure of the Mo.S.E. barriers has to be decided based on storm surge prediction at locations within the lagoon (e.g., PS and Chioggia); however, the Mo.S.E. barriers act to make peak values disappear from the time series of inner SLs.

The results reported in Fig. 8, referring to the SL gauges of PS, Chioggia, and Burano, show the SL computed by WWTM simulating the real closures of the Mo.S.E. barriers (blue lines) and the non-regulated scenario (red lines). Model results are compared with the observed SLs (black lines) showing a good agreement in the present regulated
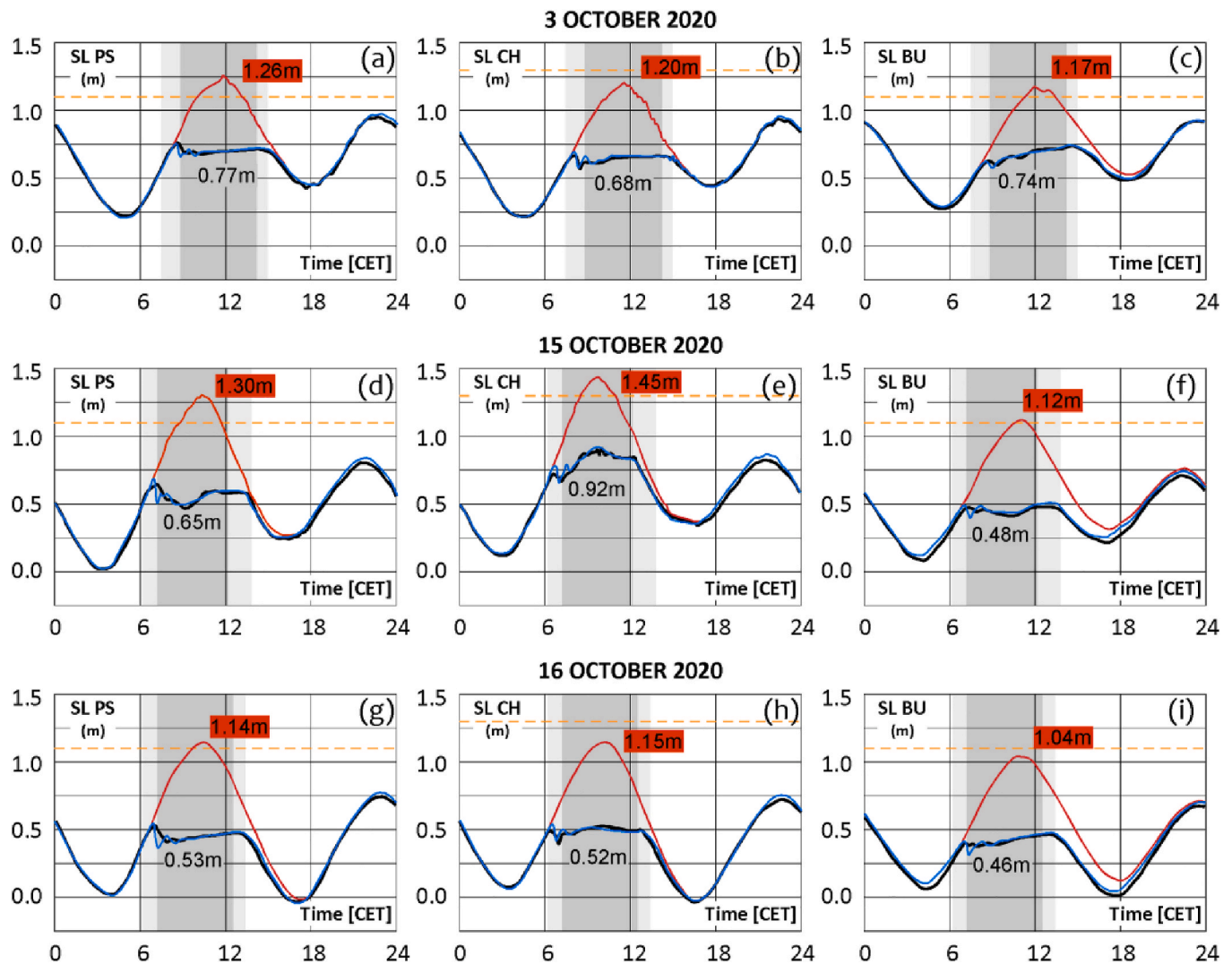
Fig. 8. Events of 3 (a)–(c), 15 (d)–(f), and 16 (g)–(i) October 2020. Comparison between SLs observed at the CPSM gauges of PS, Chioggia (CH) and Burano (BU) (black lines) and SLs computed by the WWTM model forcing the closure of the Mo.S.E. barriers (blue lines). Red lines represent the SLs computed by means of the WWTM model assuming a non-regulated scenario. Orange dashed lines represent the safeguard thresholds (1.10 m at PS and Burano and 1.30 m at Chioggia). Labels indicate, respectively, the SL peaks gauged (black) and computed by the model without forcing the closure of the inlets (red). (For interpretation of the references to colour in this figure legend, the reader is referred to the Web version of this article.)

scenarios. Blue lines often overlap with black lines, thus confirming the robust calibration of WWTM, and of the wind stress model in particular.

Each event is characterized by a SL peak, computed at PS in non-regulated conditions, higher than 1.10 m, which corresponds to the safeguard threshold above which the barriers, once fully operational, will be closed. However, the model results showed that only on 15 October the SL would have exceeded 1.30 m, i.e., the threshold adopted in the current testing phase. In particular, the official forecast of 16 October overestimated the SL at PS of about 0.15 m with a lead time of 6 h; this highlights the need of a more reliable SL prediction to prevent both missed and false alarms, particularly during the fully operational stage, when the use of the Mo.S.E. system will be more frequent.

3.3.2. The level within the lagoon is not equal to the level outside the inlets

Our findings demonstrated that the SL peaks that would have been reached within the lagoon in the hypothetical non-regulated scenario, are lower than the peaks gauged seaward at the inlets. As an example, on 3 October 2020, the Diga Sud Lido station gauged a SL peak of 1.32 m, versus a peak of 1.26 m computed at PS station by simulating the barriers kept open (lower than the threshold adopted in the current testing phase of 1.30 m – see Fig. 8a).

An analysis of the tidal observations of the period 2015–2019 demonstrated that the above occurrence is not a rare event. Considering only storm events in which the safeguard threshold of 1.10 m was exceeded at Diga Sud Lido or at Diga Sud Chioggia (Fig. 9), we compared the difference of SL peaks observed between the seaward gauge of Diga Sud Lido and the lagoonal gauge of PS (blue bars), and between Diga Sud Chioggia and Chioggia (green bars). In both cases, higher SL peaks (0.03–0.04 m on average) were recorded at the seaward stations with respect to the corresponding lagoonal stations, a direct consequence of tide propagation. Using average SLs within the lagoon and average SLs outside the inlets provides analogous results. Notably, out of the selected 65 events in which the SL exceeded the threshold of 1.10 m at the seaward stations, in 20 cases the same threshold wasn't reached at PS. This confirms that, in case of closure of the Mo.S.E. barriers, a correct assessment of the SLs that would have been recorded at the lagoonal settlements with open inlets does require the use of suitable mathematical models.

3.3.3. The cross-lagoon wind setup is enhanced when the inlets are closed

Importantly, the calibrated WWTM confirmed that the wind setup within the Venice Lagoon is much enhanced when the lagoon is
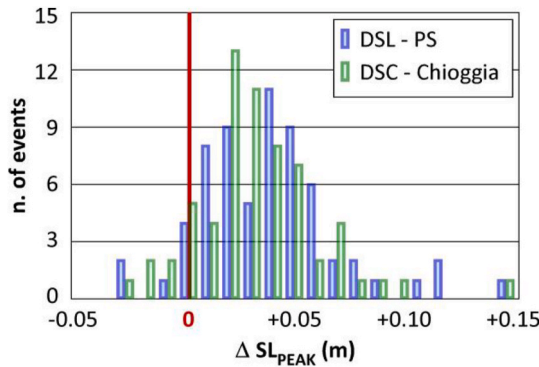
Fig. 9. Period 2015–2019: analysis of storm events in which the SL peak exceeded the threshold of 1.10 m at the seaward gauges of Diga Sud Lido or Diga Sud Chioggia. Difference of peak levels between Diga Sud Lido and PS (blue bars) and between Diga Sud Chioggia and Chioggia (green bars). (For interpretation of the references to colour in this figure legend, the reader is referred to the Web version of this article.)

temporarily closed. Looking, for example, at the storm event of 15 October (Fig. 10a), the wind setup between PS and Chioggia, ΔSL, was up to three times larger during the closure of the Mo.S.E. barriers (red bullets) than in the non-regulated scenario (light blue diamonds). Notably, a similar ΔSL ratio between scenarios with open and closed inlets was found by Mel et al. (2019a), a prior-to-Mo.S.E. study in which the regulated condition was a "what if" hypothetical scenario (see the simulation of the 10 November 2004 Bora event, reported in Fig. 3 therein).

When the same data of Fig. 10a are plotted against the wind speed (Fig. 10b), a positive correlation is found for both cases. The wind setup in the basin between PS and Chioggia, for closed inlets, is consistent with the theoretical values (black line) obtained according to Fitzgerald (1963) as $\Delta SL_T = n\, \tau_{WIND}\, L/(g\, \rho\, H_m)$, in which $L = 25$ km is the basin length, $H_m = 4$ m is the mean water depth, g is gravity, ρ is the water density, and n is a function of the ratio of bottom to wind stresses, assumed equal to 1.25 according to Keulegan (1951). The same consistency is obtained by considering the effect of wind setup as proposed by Mel et al. (2019b) for the Venice Lagoon (red line). Fig. 10b further confirms that the three inlets of the Venice Lagoon act to dampen the wind setup, particularly in the case of higher winds. Between 8:40CET and 9:40CET of 15 October, with the lagoon temporarily closed, the recorded ΔSL exceeded 0.40 m, in agreement with the values predicted

by Mel et al. (2019b) for a wind speed of about 16 m/s.

Finally, note that part of the setup computed in non-regulated conditions (say 0.05 m out of the 0.20 m reached by the light blue), is due to the SL gradient between Diga Sud Chioggia and Diga Sud Lido (i.e., at open sea; see the brown line in Figure S.4).

### 3.3.4. Mo.S.E.–induced disturbances in the northern Adriatic Sea

The SLs recorded at sea gauges during the three closures of the Mo.S. E. barriers in October 2020 (Figs. 3a, 4a and 5a) showed some anomalies, such as flattening of the tide peaks and unexpected spikes, suggesting that the closure of the Mo.S.E. barriers potentially produce some hydrodynamic effects also outside the gates and, possibly, in the northern Adriatic Sea. Indeed, it is already known that rapid changes in the wind climate (Heaps, 1983; Lionello et al., 2005) or in the air pressure gradient (Donn and Wolf, 1972) can cause the formation of long waves in the Adriatic Sea.

To investigate this issue, we simulated with the WWTM model a semi-diurnal sinusoidal tide of 0.70 m, imposed as a boundary condition in the Adriatic Sea about 100 km South of Trieste (Fig. 1), with no wind action. We performed a run with no-Mo.S.E. scenario, reproducing the non-regulated configuration of the lagoon, and a run with the Mo.S.E. closure, in which the barriers are supposed to close in 1 h at half of the rising tide (in agreement with the three events of October 2020). The comparison of SLs obtained in the two scenarios suggests that the closure of the inlets triggers a local, temporary SL increase close to the barriers, caused by the sudden reduction of fluxes entering the Lagoon, and a succeeding SL decrease (Fig. 11a). The positive wave triggered by the closure of the barriers propagates in the Northern Adriatic Sea, reflects on the coasts to assume a quite irregular pattern, then rapidly vanishes (Figure S.6 in the Supplementary material). The sea largely limits the amplitude of the positive surge compared to an open-channel case (Viero et al., 2017); according to the model, the initial amplitude of up to 25 cm in front of the Mo.S.E. barriers reduces to about 6 cm beside the inlet jetties, at the SL gauging stations, and to about 4 cm at the eastside of the Adriatic Sea (Gulf of Trieste). Additional simulations, not shown here, suggested that a different velocity in raising the Mo.S.E. gates or a slight variation of the tidal amplitude do not significantly affect these results.

For all the seaside stations, the SLs measured in the first 12 h after each of the three closure events where filtered with a 20 min weighted moving average and approximated with a sinusoidal function. The difference between measured and approximated SLs (thin lines in Fig. 11b–d) show quite an irregular pattern, possibly driven by extremely variable meteorological conditions, although with some
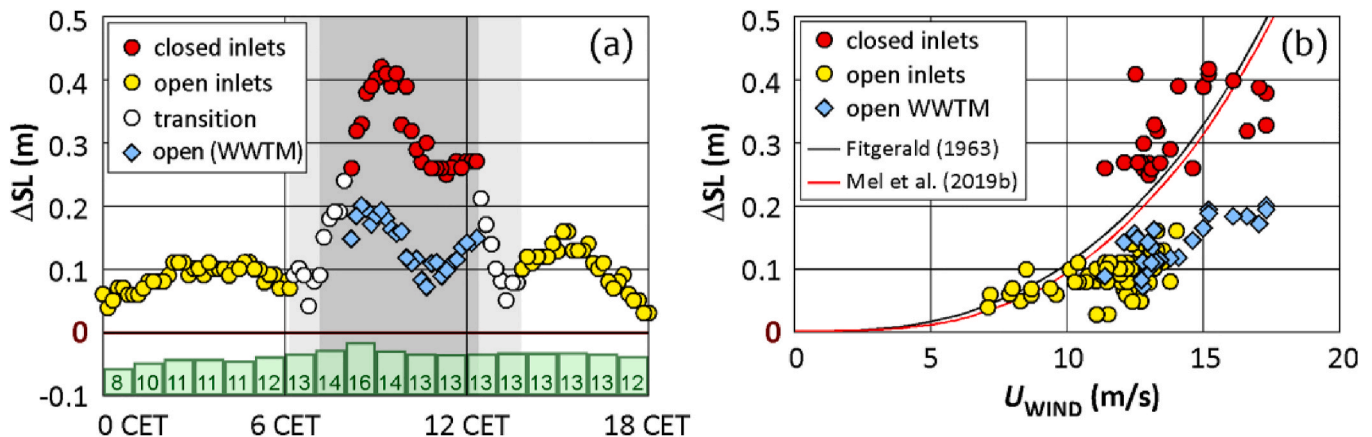
Fig. 10. Wind setup between PS and Chioggia, measured on 15 October 2020 (yellow, white, and red bullets), and simulated with WWTM with no Mo.S.E. closure (light blue diamonds). Wind setup in non-regulated periods is computed by correcting PS data for phase shift due to tide propagation (20 min). (a) Comparison of the wind setup between 00 CET and 18 CET, with green bottom bars denoting the wind speed (in m/s); (b) scatter plot of wind speed and wind setup within the same time window compared to the theoretical values obtained by Fitgerald (1963) (black) and Mel et al. (2019b) (red). (For interpretation of the references to colour in this figure legend, the reader is referred to the Web version of this article.)
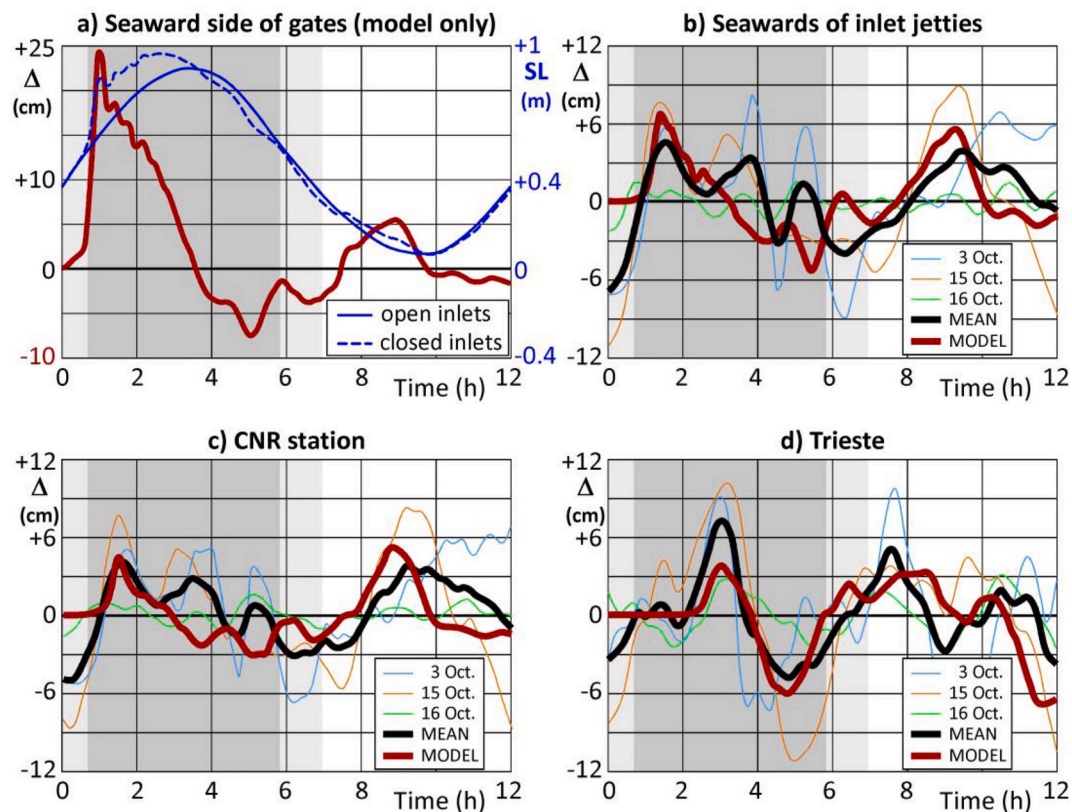
Fig. 11. Mo.S.E.-induced disturbance at the seaward side of the gates (a), just outside the three inlets (b), at the CNR (c) and Trieste (d) gauging stations. Model results refer to a synthetic scenario (sinusoidal semidiurnal tide) with a standard closure of the Mo.S.E. gates. Modelled and measured data are aligned at the beginning of Mo.S.E. closure. The red thick line denotes the SL difference between closure and no-closure modelled scenarios. In panels b, c, and d, Δ is obtained as the difference between the measured SL and its sinusoidal approximation in the 12 h after the closure. (For interpretation of the references to colour in this figure legend, the reader is referred to the Web version of this article.)

common trends. This becomes evident looking at average values (black thick lines): the disturbance in measured and modelled data show major peaks characterized by similar magnitude, and a very similar timing, outside the lagoon inlets, at the CNR station, and at Trieste as well (Fig. 11b–d). This suggests that the Mo.S.E. actually induces some disturbance at the seaside, and that this disturbance propagates in the Northern Adriatic Sea in the form of a long, small-amplitude wave, as predicted by the WWTM model.

4. Conclusions

In the present study, we analyzed from a hydrodynamic point of view the first three operations of the Mo.S.E. barriers that, in October 2020, have temporarily closed the Venice Lagoon to prevent Venice and the other urban settlements within the lagoon from flooding. This unique occurrence gave us the chance of analyzing specific issues using unprecedented data. Specifically:

- a first quantitative estimate was obtained for the intra-gate infiltration, i.e., the flow rate that enters the lagoon through the movable gates, causing a not negligible raising of sea level within the lagoon during long closure periods. For the cases we analyzed, we obtained a total flow rate entering the lagoon during the closure of more than 1000 m³/s, corresponding to ~1 cm/h of sea level raising rate;
- a robust calibration of the wind drag coefficient was achieved also for moderate wind speed, as in the closed lagoon the wind setup is not masked by the propagation of the tidal wave. In shallow water conditions, the best-fitting drag coefficient increases linearly with the wind speed at a rate that is larger than for the open ocean, as suggested by previous studies and supported by the recent literature;

- the ex-post analysis of the three closure events, based on the calibrated hydrodynamic model WWTM, showed that the cross-lagoon wind setup is magnified when the lagoon is temporarily closed thus confirming that, in the non-regulated scenario, the fluxes through the three inlets adjust to reduce the gradient of inner sea levels;
- model simulations allowed to reconstruct the sea levels that would have been recorded within the lagoon in the hypothetical scenario of no Mo.S.E. operation, which is important for several reasons (see Section 3.3.1) and, in particular, considering that the closure of the Mo.S.E. barriers has to be decided based on the level forecast within the lagoon. We highlighted that sea level peaks within the lagoon are generally different (and typically lower) than those recorded outside the lagoon inlets, with direct implications on minimizing and detecting possible missed and false alarms;
- measured and modelled sea level data showed that the closure of the Mo.S.E. barriers causes some hydrodynamic disturbance at the seaward side as well. In particular, during the Mo.S.E. closure, the sea level increases of up to 25 cm in front of the gates and to less than 10 cm out of the inlet jetties. This local disturbance triggers a long, small-amplitude wave that propagates in the Northern Adriatic Sea undergoing multiple reflections on the coasts and vanishing in few hours.

Besides this first attempt to study some major hydrodynamic issues that emerged during the first operations of the Mo.S.E. barriers, many other open issues remain to be analyzed as, for example, the long-term influence of the closures on the bio-morphodynamic evolution of the Venice Lagoon. The next Mo.S.E. closures will further help the hydrodynamic insights of a regulated lagoon, where ad hoc field

measurements are recommended.

Declaration of competing interest

The authors declare that they have no known competing financial interests or personal relationships that could have appeared to influence the work reported in this paper.

Acknowledgments

Appendix A. Supplementary data

Supplementary data to this article can be found online at https://doi.org/10.1016/j.ecss.2021.107547.

Funding

Author contributions

R.A. Mel: conceptualization, data curation, investigation, methodology, software, validation, visualization, writing original draft; **D.P. Viero**: conceptualization, methodology, software, visualization, writing review & editing; **L. Carniello**: conceptualization, methodology, software, supervision, writing review & editing; **A. Defina**: conceptualization, methodology, writing review & editing; **L. D'Alpaos**: methodology, supervision, writing review & editing.

References

Bajo, M., Zampato, L., Umgiesser, G., Cucco, A., Canestrelli, P., 2007. A finite element operational model for storm surge prediction in Venice. Estuar. Coast Shelf Sci. 75 (1–2), 236–249. https://doi.org/10.1016/j.ecss.2007.02.025.

Bajo, M., Umgiesser, G., 2010. Storm surge forecast through a combination of dynamic and neural network models. Ocean Model. 33 (1–2), 1–9. https://doi.org/10.1016/j.ocemod.2009.12.007.

Bertagnoli, G., Anerdi, C., Malavisi, M., Zoratto, N., 2017. Autogenous crack control during ConstructionPhases of MOSE Venice dams. IOP Conf. Ser. Mater. Sci. Eng. 245 (2), 022080 https://doi.org/10.1088/1757-899X/245/2/022080.

Bi, X., Gao, Z., Liu, Y., Liu, F., Song, Q., Huang, J., Huang, H., Mao, W., Liu, C., 2015. Observed drag coefficients in high winds in the near offshore of the South China Sea. J. Geophys. Res. Atmos. 120, 6444–6459. https://doi.org/10.1002/2015JD023172.

Brambati, A., Carbognin, L., Quaia, T., Teatini, P., Tosi, L., 2003. The Lagoon of Venice: geological setting, evolution and land subsidence. Episodes 26 (3), 264–268. https://doi.org/10.18814/epiiugs/2003/v26i3/020.

Bryant, K.M., Akbar, M., 2016. An exploration of wind stress calculation techniques in hurricane storm surge modeling. J. Mar. Sci. Eng. 4, 58. https://doi.org/10.3390/jmse4030058.

Carbognin, L., Teatini, P., Tomasin, A., Tosi, L., 2010. Global change and relative sea level rise at Venice: what impact in term of flooding. Clim. Dynam. 35, 1039–1047. https://doi.org/10.1007/s00382-009-0617-5.

Carniello, L., Defina, A., Fagherazzi, S., D'Alpaos, L., 2005. A combined wind wave-tidal model for the Venice lagoon, Italy. J. Geophys. Res. Earth Surf. 110, F04007. https://doi.org/10.1029/2004JF000232.

Carniello, L., D'Alpaos, A., Defina, A., 2011. Modeling wind waves and tidal flows in shallow micro-tidal basins. Estuar. Coast Shelf Sci. 92 (2), 263–276. https://doi.org/10.1016/j.ecss.2011.01.001.

Carniello, C., Defina, A., D'Alpaos, L., 2009. Morphological evolution of the Venice Lagoon: evidence from the past and trend for the future. J. Geophys. Res. Earth Surf. 114, F04002. https://doi.org/10.1029/2008JF001157.

Carniello, L., Defina, A., D'Alpaos, L., 2012. Modeling sand-mud transport induced by tidal currents and wind waves in shallow microtidal basins: application to the Venice Lagoon (Italy). *Estuar. Coast. Shelf Sci.* 102– 103, 105–115. https://doi.org/10.1016/j.ecss.2012.03.016.

Cavaleri, L., Bajo, M., Barbariol, F., Bastianini, M., Benetazzo, A., Bertotti, L., Chiggiato, J., Ferrarin, C., Trincardi, F., Umgiesser, G., 2020. The 2019 flooding of

Venice and its implications for future predictions. Oceanography 33, 42–49. https://doi.org/10.5670/oceanog.2020.105.

Cavallaro, L., Iuppa, C., Foti, E., 2017. Effect of partial use of Venice flood barriers. J. Mar. Sci. Eng. 5 (4), 58. https://doi.org/10.3390/jmse5040058.

Cerovečki, I., Orlić, M., Herdershott, M., 1997. Adriatic seiche decay and energy lost to the Mediterranean. Deep Sea Res. Part I 44 (12), 2007–2029. https://doi.org/10.1016/S0967-0637(97)00056-3.

Charnock, H., 1955. Wind stress on a water surface. Quart. J. Roy. Meteor. Soc. 81, 639–640. https://doi.org/10.1002/qj.49708135027.

Chen, S., Qiao, F., Jiang, W., Guo, J., Dai, D., 2019. Impact of surface waves on wind stress under low to moderate wind conditions. J. Phys. Oceanogr. 49 (8), 2017–2028. https://doi.org/10.1175/JPO-D-18-0266.1.

Comune di Venezia, 2020. Previsioni delle altezze di marea per il bacino San Marco. Annual publication, p. 72 (in Italian).

Consorzio Venezia Nuova, 2003. Studio sugli effetti di scala nelle prove su modello fisico delle paratoie, 2.5 valutazione della portata transitante nei traferri delle paratoie. Magistrato alle Acque di Venezia B 6 (53), 232.

Consorzio Venezia Nuova, 2006. Studio di particolari aspetti idrodinamici delle paratoie attraverso prove su modelli fisici – II fase: misura delleportate attraverso lo sbarramento e delle forze trasmesse alla fondazione. Magistrato alle Acque di Venezia B.06.08/II, p. 224.

D'Alpaos, A., Carniello, L., Mudd, S.M., 2011. Dynamic response of marshes to perturbations in suspended sediment concentrations and rates of relative sea level rise. J. Geophys. Res. Earth Surf. 116, F04020. https://doi.org/10.1029/2011JF002093.

D'Alpaos, L., Defina, A., 1993. Venice lagoon hydrodynamics simulation by coupling 2D and 1D finite element models. In: In: *Proceedings Of the 8th Conference On Finite Elements In Fluids*, New Trends and Applications, Pp. 917–926, Barcelona, 20-24 September.

D'Alpaos, L., Defina, A., 2007. Mathematical modeling of tidal hydrodynamics in shallow lagoons: a review of open issues and applications to the Venice lagoon. Comput. Geosci. 33, 476–496. https://doi.org/10.1016/j.cageo.2006.07.009.

D'Alpaos, L., 2010. Fatti e misfatti di idraulica lagunare. La laguna di Venezia dalla diversione dei fiumi alle nuove opere delle bocche di porto. Istituto Veneto di Scienze, Lettere e Arti, Venice, ISBN 9788895996219.

Del Bello, L., 2019. Venice anti-flood gates could wreck lagoon ecosystem. Nature 564, 16. https://doi.org/10.1038/d41586-018-07372-3.

Defina, A., 2000. Two dimensional shallow flow equations for partially dry areas. Water Resour. Res. 36 (11), 3251–3264. https://doi.org/10.1029/2000WR900167.

Defina, A., 2003. Numerical experiments on bar growth. Water Resour. Res. 39 (4) https://doi.org/10.1029/2002WR001455.

Donelan, M., 1982. The dependence of the aerodynamic drag coefficient on wave parameters. *Proc. First Int. Conf. On Meteorology And Air-Sea Interaction In the Coastal Zone*, the Hague. Amer. Meteor. Soc., pp. 381–387

Donelan, M.A., Haus, B.K., Reul, N., Plant, W.J., Stiassnie, M., Graber, H.C., Brown, O.B., Saltzman, E.S., 2004. On the limiting aerodynamic roughness of the ocean in very strong winds. Geophys. Res. Lett. 31 (18), L18306. https://doi.org/10.1029/2004GL019460.

Donn, W.L., Wolf, D.M., 1972. Seiche and water level fluctuations in Grindavik Harbor. Iceland. *Limnol. Oceanogr.* 17, 639–643. https://doi.org/10.4319/lo.1972.17.4.0639.

Edson, J., Jampana, V., Weller, R.A., Bigorre, S.P., Plueddemann, A.J., Fairall, C.W., Miller, S.D., Mahrt, L., Vickers, D., Hersbach, H., 2013. On the exchange of momentum over the open ocean. J. Phys. Oceanogr. 43 (8), 1589–1610. https://doi.org/10.1175/JPO-D-12-0173.1.

Eprim, Y., 2005. Venice mobile barriers project: barrier caissons construction details. In: Fletcher, C.A., Spencer, T. (Eds.), Flooding and Environmental Challenges for Venice and its Lagoon: State of Knowledge. Cambridge University Press, Cambridge, pp. 257–265.

Fagherazzi, S., Wiberg, P.L., 2009. Importance of wind conditions, fetch, and water levels on wave-generated shear stresses in shallow intertidal basins. J. Geophys. Res. Earth Surf. 114 (F3), F03022. https://doi.org/10.1029/2008JF001139.

Ferrarin, C., Valentini, A., Vodopivec, M., Klaric, D., Massaro, G., Bajo, M., De Pascalis, F., Fadini, A., Ghezzo, M., Menegon, S., Bressan, L., Unguendoli, S., Fettich, A., Jerman, J., Ličer, M., Fustar, L., Papa, A., Carraro, E., 2020. Integrated sea storm management strategy: the 29 October 2018 event in the Adriatic Sea. Nat. Hazards Earth Syst. Sci. 20, 73–93. https://doi.org/10.5194/nhess-20-73-2020.

Fitzgerald, L.M., 1963. Wind-induced stresses on water surfaces. A wind-tunnel study. Aust. J. Phys. 16, 475–489. https://doi.org/10.1071/PH630475.

Heaps, N.S., 1983. Storm surges, 1967–1982. Geophys. J. Int. 74 (1), 331–376. https://doi.org/10.1111/j.1365-246X.1983.tb01883.x.

International College of Experts, 1998. In: Report on the mobile gates project for the tidal flow regulation at the Venice lagoon inlets (members: P. Bourdeau, J.M. Martin, C.C. Mei, I. Musu, P. Vellinga). In: Numero speciale dei Quaderni Trimestrali, Venezia, Italia.

IPCC, 2013. Annex II: climate system scenario tables. In: Prather, M., Flato, G., Friedlingstein, P., Jones, C., Lamarque, J.-F., Liao, H., Rasch, P. (Eds.), Climate Change 2013: the Physical Science Basis. Contribution of Working Group I to the Fifth Assessment Report of the Intergovernmental Panel on Climate Change. Cambridge University Press, Cambridge, United Kingdom and New York, NY, USA.

Janssen, P.A.E.M., 1989. Wave-induced stress and the drag of air flow over sea waves. J. Phys. Oceanogr. 19 (6), 745–754. https://doi.org/10.1175/1520-0485(1989)019<0745:WISATD>2.0.CO;2.

Jiménez, P.A., Dudhia, J., 2018. On the need to modify the sea surface roughness formulation over shallow waters. J. Appl. Meteorol. Clim. 57 (5), 1101–1110. https://doi.org/10.1175/JAMC-D-17-0137.1.

Keulegan, G.H., 1951. Wind tides in small closed channels. J. Res. Natl. Bur. Stand. (U.S.) 46 (5), 358–381. https://doi.org/10.6028/jres.046.041.

Kim, S.-Y., Hong, S.-Y., Kwon, Y.C., Lee, Y.H., Kim, D.-E., 2019. Effects of Modified Surface Roughness Length over Shallow Waters in a Regional Model Simulation. Atmosphere 10, 818. https://doi.org/10.3390/atmos10120818.

Large, W.G., Pond, S., 1981. Open ocean momentum flux measurements in moderate to strong winds. J. Phys. Oceanogr 11 (3), 324–336. https://doi.org/10.1175/1520-0485(1981)011<0324:OOMFMI>2.0.CO;2.

Lionello, P., Mufato, R., Tomasin, A., 2005. Sensitivity of free and forced oscillations of the Adriatic Sea to sea level rise. Clim. Res. 29 (1), 23–39. https://doi.org/10.3354/cr029023.

Lionello, P., 2012. The climate of the Venetian and North Adriatic region: variability, trends and future change. Phys. Chem. Earth. Parts A/B/C 40– 41, 1–8. https://doi.org/10.1016/j.pce.2012.02.002.

Mahrt, L., Andreas, E.L., Edson, J.B., Vickers, D., Sun, J., Patton, E.G., 2016. Coastal zone surface stress with stable stratification. J. Phys. Oceanogr. 46 (1), 95–105. https://doi.org/10.1175/JPO-D-15-0116.1.

Marcos, M., Tsimplis, M.N., Shaw, A.G.P., 2009. Sea level extremes in southern Europe. J. Geophys. Res. 144, C01007. https://doi.org/10.1029/2008JC004912.

Mariotti, G., Fagherazzi, S., Wiberg, P., McGlathery, K., Carniello, L., Defina, A., 2010. Influence of storm surges and sea level on shallow tidal basin erosive processes. J. Geophys. Res. Oceans 115, C11012. https://doi.org/10.1029/2009JC005892.

Martini, P., Carniello, L., Avanzi, C., 2004. Two dimensional modelling of flood flows and suspended sedimenttransport: the case of the Brenta River, Veneto (Italy). Nat. Hazards Earth Syst. Sci. 4, 165–181. https://doi.org/10.5194/nhess-4-165-2004.

Matticchio, B., Carniello, L., Canesso, D., Ziggiotto, E., Cordella, M., 2017. Recenti variazioni della propagazione della marea in Laguna di Venezia: effetti indotti dalle opere fisse alle Bocche di Porto. In: D'Alpaos, L. (Ed.), Commissione di studio sui problemi di Venezia, Volume III: La laguna di Venezia e le nuove opere alle bocche. Istituto Veneto di Scienze, Lettere ed Arti, ISBN 978-88-95996-77-6, pp. 157–183.

Mel, R., Sterl, A., Lionello, P., 2013. High resolution climate projection of storm surge at the Venetian coast. Nat. Hazards Earth Syst. Sci. 13, 1135–1142. https://doi.org/10.5194/nhess-13-1135-2013.

Mel, R., Lionello, P., 2014. Storm surge ensemble prediction for the city of Venice. Weather Forecast. 29 (4), 1044–1057. https://doi.org/10.1175/WAF-D-13-00117.1.

Mel, R., Viero, D.P., Carniello, L., Defina, A., D'Alpaos, L., 2014. Simplified methods for real-time prediction of storm surge uncertainty: the city of Venice case study. Adv. Water Resour. 71, 177–185. https://doi.org/10.1016/j.advwatres.2014.06.014.

Mel, R., D'Alpaos, L., 2017. Sui sovralzi dei colmi di marea generati dal vento nella laguna di Venezia a causa della chiusura delle paratoie mobili alle Bocche di Porto. Commissione di studio sui problemi di Venezia, Volume III: La laguna di Venezia e le nuove opere alle bocche. Istituto Veneto di Scienze, Lettere e Arti, Venezia.

Mel, R., Carniello, L., D'Alpaos, L., 2019a. Addressing the effect of the Mo.S.E. barriers closure on wind setup within the Venice lagoon. Estuar. Coast Shelf Sci. 225, 106249. https://doi.org/10.1016/j.ecss.2019.106249.

Mel, R., Carniello, L., D'Alpaos, L., 2019b. Dataset of wind setup in a regulated Venice lagoon. Data Br 26, 104386. https://doi.org/10.1016/j.dib.2019.104386.

Mel, R., Carniello, L., D'Alpaos, L., 2021. How long the Mo.S.E. barriers will be effective in protecting all urban settlements within the Venice Lagoon? The wind setup constraint. Coast. Eng. 168. https://doi.org/10.1016/j.coastaleng.2021.103923, 103923.

Molinaroli, E., Guerzoni, S., Suman, D., 2019. Do the adaptations of Venice and miami to sea level rise offer lessons for other vulnerable coastal cities? Environ. Man 64, 391–415. https://doi.org/10.1007/s00267-019-01198-z.

Ortiz-Suslow, D.G., Haus, B.K., Williams, N.J., Laxague, N.J.M., Reniers, A.J.H.M., Graber, H.C., 2015. The spatial-temporal variability of air-sea momentum fluxes observed at a tidal inlet. J. Geophys. Res. Oceans 120, 660–676. https://doi.org/10.1002/2014JC010412.

Ortiz-Suslow, D.G., Haus, B.K., Williams, N.J., Graber, H.C., MacMahan, J.H., 2018. Observations of air-sea momentum flux variability across the inner shelf. J. Geophys. Res. Oceans 123, 8970–8993. https://doi.org/10.1029/2018JC014348.

Pareja-Roman, L.F., Chant, R.J., Ralston, D.K., 2019. Effects of locally generated wind waves on the momentum budget and subtidal exchange in a coastal plain estuary. J. Geophys. Res. Oceans 124, 1005–1028. https://doi.org/10.1029/2018JC014585.

Pasarić, Z., Belušić, D., Chiggiato, J., 2009. Orographic effects on meteorological fields over the Adriatic from different models. J. Mar. Syst. 78, S90–S100. https://doi.org/10.1016/j.jmarsys.2009.01.019.

Pirazzoli, P.A., 2002. Did the Italian Government approve an obsolete project to save Venice? Eos 83 (20), 217–223. https://doi.org/10.1029/2002EO000148.

Pivato, M., Carniello, L., Viero, D.P., Soranzo, C., Defina, A., Silvestri, S., 2020. Remote sensing for optimal estimation of water temperature dynamics in shallow tidal environments. Rem. Sens. 12 (1), 51. https://doi.org/10.3390/rs12010051.

Porchetta, S., Temel, O., Muñoz-Esparza, D., Reuder, J., Monbaliu, J., van Beeck, J., van Lipzig, N., 2019. A new roughness length parameterization accounting for wind–wave (mis) alignment. Atmos. Chem. Phys. 19, 6681–6700. https://doi.org/10.5194/acp-19-6681-2019.

Reimann, L., Vafeidis, A.T., Brown, S., Hinkel, J., Tol, R.S.J., 2018. Mediterranean UNESCO World Heritage at risk from coastal flooding and erosion due to sea-level rise. Nat. Commun. 9, 4161. https://doi.org/10.1038/s41467-018-06645-9.

Rinaldo, A., Nicotina, L., Alessi Celegon, E., Beraldin, F., Botter, G., Carniello, L., Cecconi, G., Defina, A., Settin, T., Uccelli, A., D'Alpaos, L., Marani, M., 2008. Sea level rise, hydrologic runoff, and the flooding of Venice. Water Resour. Res. 44, 12. https://doi.org/10.1029/2008WR007195.

Rizzi, J., Torresan, S., Zabeo, A., Critto, A., Tosoni, A., Tomasin, A., Marcomini, A., 2017. Assessing storm surge risk under futuresea-level rise scenarios: a case study in the North Adriatic coast. J. Coast Conserv. 21, 453–471. https://doi.org/10.1007/s11852-017-0517-5.

Ruol, P., Favaretto, C., Volpato, M., Martinelli, L., 2020. Flooding of piazza san marco (Venice): physical model tests to evaluate the overtopping discharge. Water 12, 427. https://doi.org/10.3390/w12020427.

Ruol, P., Martinelli, L., Favaretto, C., 2018. Vulnerability analysis of the Venetian littoral and adopted mitigation strategy. Water 10, 984. https://doi.org/10.3390/w10080984.

Scarascia, L., Lionello, P., 2013. Global and regional factors contributing to the past and future sea level rise in the Adriatic Sea. Global Planet. Change 106, 51–63. https://doi.org/10.1016/j.gloplacha.2013.03.004.

Shabani, B., Nielsen, P., Baldock, T., 2014. Direct measurements of wind stress over the surf zone. J. Geophys. Res. Oceans 119, 2949–2973. https://doi.org/10.1002/2013JC009585.

Silvestri, S., D'Alpaos, A., Nordio, G., Carniello, L., 2018. Anthropogenic modifications can significantly influence the local mean sea level and affect the survival of salt marshes in shallow tidal systems. J. Geophys. Res. Earth Surf. 123 (5), 996–1012. https://doi.org/10.1029/2017JF004503.

Smith, S.D., 1980. Wind stress and heat flux over the ocean in gale force winds. J. Phys. Oceanogr. 10, 709–726. https://doi.org/10.1175/1520-0485(1980)010<0709:WSAHFO>2.0.CO, 1980,2.

Smith, S.D., Banke, E.G., 1975. Variation of the sea surface drag coefficient with wind speed. Q. J. R. Meteorol. Soc. 101, 665–673. https://doi.org/10.1002/qj.49710142920.

Smith, S.D., Anderson, R.J., Oost, W.A., Kraan, C., Maat, N., De Cosmo, J., Katsaros, K.B., Davidson, K.L., Bumke, K., Hasse, L., Chadwick, H.M., 1992. sea surface wind stresses and drag coefficients: the HEXOS program. Bound.-Lay. Meteorol. 60, 109–142. https://doi.org/10.1007/BF00122064.

Sterl, A., 2017. Drag at high wind velocities – a review. Roy. Netherland Met. Office. Tech. Rep. 361, 23.

Tognin, D., Pivato, M., D'Alpaos, A., Carniello, L., 2020. How do storm events and fair-weather conditions affect sedimentation patterns on salt marshes? EGU General Assembly 2020, EGU2020–10828. https://doi.org/10.5194/egusphere-egu2020-10828.

Tognin, D., D'Alpaos, A., Marani, M., Carniello, L., 2021. Coastal Flooding Protection vs. Salt-Marsh Survival: a Short-Blanket Syndrome submitted for publication.

Trincardi, F., Barbanti, A., Bastianini, M., Benetazzo, A., Cavaleri, L., Chiggiato, J., Papa, A., Pomaro, A., Sclavo, M., Tosi, L., Umgiesser, G., 2016. The 1966 flooding of Venice: what time taught us for the future. Oceanography 29, 178–186. https://doi.org/10.5670/oceanog.2016.87, 2016.

Umgiesser, G., Melaku Canu, D., Cucco, A., Solidoro, C., 2004. A finite element model for the Venice Lagoon.Development, set up, calibration and validation. J. Mar. Syst. 51, 123–145. https://doi.org/10.1016/j.jmarsys.2004.05.009.

Umgiesser, G., Matticchio, B., 2006. Simulating the mobile barrier (MOSE) operation in the Venice Lagoon, Italy: global sea level rise and its implication for navigation. Ocean Dynam. 56, 320–332. https://doi.org/10.1007/s10236-006-0071-4.

Umgiesser, G., 2020. The impact of operating the mobile barriers in Venice (MOSE) under climate change. J. Nat. Conserv. 54, 125783. https://doi.org/10.1016/j.jnc.2019.125783.

Vickers, D., Mahrt, L., 1997. Fetch limited drag coefficients. Bound.-Lay. Meteorol. 85, 53–79. https://doi.org/10.1023/A:1000472623187.

Viero, D.P., D'Alpaos, L., Carniello, L., Defina, A., 2013. Mathematical modeling of flooding due to river bank failure. Adv. Water Resour. 59, 82–94. https://doi.org/10.1016/j.advwatres.2013.05.011.

Viero, D.P., Defina, A., 2016. Water age, exposure time, and local flushing time in semi-enclosed, tidal basins with negligible freshwater inflow. J. Mar. Syst. 156, 16–29. https://doi.org/10.1016/j.jmarsys.2015.11.006.

Viero, D.P., Peruzzo, P., Defina, A., 2017. Positive surge propagation in sloping channels. Water 9 (7), 518. https://doi.org/10.3390/w9070518.

Zampato, L., Umgiesser, G., Zecchetto, S., 2007. Sea level forecasting in Venice through high resolution meteorological fields. Estuar. Coast Shelf Sci. 75 (1–2), 223–235. https://doi.org/10.1016/j.ecss.2007.02.024.

Zarzuelo, C., López-Ruiz, A., D'Alpaos, A., Carniello, L., Ortega-Sánchez, M., 2018. Assessing the morphodynamic response of human-altered tidal embayments. Geomorphology 320, 127–141. https://doi.org/10.1016/j.geomorph.2018.08.014.

Zecchetto, S., Umgiesser, G., Brocchini, M., 1997. Hindcast of a storm surge induced by local real wind fields in the Venice lagoon. Continent. Shelf Res. 17 (12), 1513–1538. https://doi.org/10.1016/S0278-4343(97)00023-X.

Zhao, D., Li, M., 2019. Dependence of wind stress across an air–sea interface on wave states. J. Oceanogr. 75, 207–223. https://doi.org/10.1007/s10872-018-0494-9.

Zhao, Z.-K., Liu, C.-X., Li, Q., Dai, G.-F., Song, Q.-T., Lv, W.-H., 2015. Typhoon air-sea drag coefficient in coastal regions. J. Geophys. Res. Oceans 120, 716–727. https://doi.org/10.1002/2014JC010283.